

N O T I C E

THIS DOCUMENT HAS BEEN REPRODUCED FROM
MICROFICHE. ALTHOUGH IT IS RECOGNIZED THAT
CERTAIN PORTIONS ARE ILLEGIBLE, IT IS BEING RELEASED
IN THE INTEREST OF MAKING AVAILABLE AS MUCH
INFORMATION AS POSSIBLE

(NASA-CR-165240) ELECTROSTATIC BONDING OF
THIN (CYCLE SINE 3 MIL) 7070 COVER GLASS TO
Ta₂O₅ AR-COATED THIN (CYCLE SINE 2 MIL)
SILICON WAFERS AND SOLAR CELLS (Boeing
Aerospace Co., Seattle, Wash.) 77 p

N81-16582

Unclass
41265

G3/44

NASA CR 165240
D180-2 (200-1)



ELECTROSTATIC BONDING OF THIN (~3mil) 7070 COVER GLASS
TO Ta₂O₅ AR-COATED THIN (~2mil) SILICON WAFERS
AND SOLAR CELLS

Prepared by D. W. Egelkroun

The Boeing Company

prepared for

National Aeronautics and Space Administration

NASA Lewis Research Center
Contract NAS3-22216



FOREWORD

This report was prepared by the Boeing Aerospace Company under NASA contract NAS3-22216. The principal investigator on this program was Mr. D. W. Egelkrout. Mr. W. E. Horne was responsible for the original program instigation and planning at Boeing and gave valuable guidance and consultation throughout the effort. Other significant contributors at Boeing were Mr. C. Deminet who provided valuable expertise and assistance in the area of glass technology and Mr. D. E. Swedenburg who designed and fabricated most of the supporting electronics required to perform the research.

The author would like to thank the contract technical monitor, Ms. E. Anagnostou and also Mr. M. Forestieri of NASA Lewis Research Center for their guidance and technical support throughout this program.

ABSTRACT

This document reports the work performed at the Boeing Aerospace Company for NASA Lewis Research Center during the period from December 1979 to December 1980 on electrostatic bonding of thin cover glass to thin solar cells. Silicon solar cells, wafers, and Corning 7070 glass of from $\sim 0.002''$ to $\sim 0.003''$ in thickness were used in the investigation to establish optimum parameters for producing mechanically acceptable bonds while minimizing thermal stresses and resultant solar cell electrical parameter degradation.

TABLE OF CONTENTS

	<u>PAGE</u>
1.0 INTRODUCTION.....	1
2.0 PROCESS DESCRIPTION AND BONDING APPARATUS.....	4
2.1 THEORY.....	4
2.2 BONDING APPARATUS AND BASIC PROCEDURE.....	6
3.0 SAMPLE DESCRIPTIONS.....	10
3.1 COVER GLASS DESCRIPTIONS.....	10
3.2 SILICON WAFER DESCRIPTIONS.....	12
3.3 SOLAR CELL DESCRIPTIONS.....	12
4.0 GLASS PREPARATIONS.....	17
4.1 INITIAL CLEANING.....	17
4.2 FORMATION OF NOTCHES IN COVER GLASSES.....	17
5.0 TASK I - BONDING GLASS TO SILICON WAFERS.....	19
5.1 PRELIMINARY PROCEDURE DEVELOPMENT.....	19
5.1.1 Glass Damage.....	19
5.1.2 Determination of Degree of Bonding.....	22
5.1.3 Bonding Parameters and Bonding Approach.....	24
5.2 (T, V, t,) SURFACE DETERMINATION.....	27
5.3 AMBIENT EFFECTS.....	31
5.4 GLASS AND SILICON SURFACE TREATMENTS.....	33
5.4.1 Ta ₂ O ₅ AR-Coating Thickness.....	36
5.4.2 Ion Exchange.....	37
5.4.3 Cation Adsorption.....	39
5.4.4 Cleaning With H ₂ O ₂	39
5.5 DELIVERABLE SAMPLES/SELECTION OF OPTIMUM BONDING CONDITIONS.....	40
6.0 TASK II AND III -- BONDING GLASS TO SOLAR CELLS.....	42
6.1 PRELIMINARY ATTEMPTS AND PROBLEM DEFINITION.....	42
6.2 CATHODE-PILLOW ASSISTED BONDING.....	42
6.3 ELECTRO-OPTICALLY ASSISTED ESB.....	51
6.4 DELIVERABLE SAMPLES.....	54
7.0 CONCLUSIONS AND RECOMMENDATIONS.....	55
8.0 REFERENCES.....	58

TABLE OF CONTENTS (Continued)

	<u>PAGE</u>
APPENDIX A -- MECHANICAL-SCREENING TESTS.....	59
A.1 TEMPERATURE CYCLING.....	59
A.2 PEEL TEST.....	59
APPENDIX B -- ELECTRICAL PARAMETER MEASUREMENTS	65
APPENDIX C -- METHODS FOR FORMATION OF NOTCHES IN COVER GLASSES....	67

LIST OF FIGURES

FIGURE		PAGE
2-1	Schematic Showing Aspects of Electrostatic Bonding.....	5
2-2	Conceptual Drawing of Bonder Head.....	7
2-3	Photograph of ESB Bonder.....	8
2-4	Bonder Control and Data Acquisition System.....	9
3-1	Wafer and Glass Surface Profiles.....	11
3-2	Example Photographs of Wafer Surfaces.....	13
3-3	Solar Cell Grid Patterns.....	14
3-4	Example Surface Profiles of Solar Cells.....	15
5-1	Glass Damage Observed Using Machined Copper Cathode....	20
5-2	Examples of Glass and Cathode Damage Due to Hypothesized Discharge.....	21
5-3	Example Photomicrograph of Wafer With Glass Bonded.....	23
5-4	Example Strip Chart Records of Bonding Parameters.....	25
5-5	Electrostatic Bonding T, V, t Surface.....	28
5-6	Two-Dimensional Plots of Bonding Parameter Dependences for Wafers (\wedge Bad Bond, \vee Good Bond).....	29
5-7	Microscopic Percentage Bond Versus $\int I(t)dt$	30
5-8	Voltage Breakdown of Pure Gases as a Function of Pressure Times Spacing.....	32
5-9	Example Low Pressure Gas Breakdown Voltage Dependence..	34
5-10	Example of Bond Degree Versus Wafer Surface Coating Thickness (Using Identical Bonding Conditions).....	38
6-1	Viscosity vs. Temperature for Some Commercial Glasses..	43
6-2	Physical Features of ESB Process Using Hard and Soft Cathodes.....	44
6-3	Physical Features of Altered Bonder Head Showing Cathode Pillow and Alignment Mechanism.....	46
6-4	Example Solar Cells With Glass Bonded Using Hard and Soft Cathode.....	47

LIST OF FIGURES (Continued)

		PAGE
6-5	Example of Best Case Electrical Parameter Degradation Caused by ESB.....	49
6-6	Comparison of Microscopic Bonding Using Cathode Pillow and Laser Heating.....	53
A-1	Temperature Cycling Hardware.....	60
A-2	Functional Diagram of Temperature Cycle Controller.....	61
A-3	Example Temperature Cycle Excursions.....	62
A-4	Peel Test Hardware.....	64
B-1	Solar Cell Parameter Measurement System.....	66

LIST OF TABLES

1-1	Electrostatic Bonding Task Outline.....	3
3-1	Summary of Glass Thickness Measurements.....	10
5-1	Summary of Bonding Parameters for Delivered Wafers.....	41
6-1	Tabulation of Pre- and Post-Bond Electrical Parameter Values For Samples With $\int I(t)dt = 3 \text{ mA}\cdot\text{min}$	50

1.0 INTRODUCTION

Thin covers are needed to exploit the advantages of thin solar cells planned for use in future space missions. Glass has proven to be the best cover material over many years of use. Historically, thick glass covers have been attached to thick cells using adhesives. In order to eliminate the adhesive layer, electrostatic bonding (ESB) of Corning 7070 glass using heated covers and cells has been accomplished under Air Force Contract (ref. 1). Corning 7070 appears to have the best match of physical optical, and electrical properties for use with silicon. In previous work, ~10-mil thick cells and glass were typical. Prior to the current effort, ESB had been tried with thin (~2 to 3 mil) glass and cells; however, since the process variables had not been optimized for such samples, the results were not satisfactory. The present effort was undertaken to extend the use of the ESB process to thin cells and thin covers.

The electrostatic bonding process (also referred to as field-assisted glass-metal sealing) was first reported in 1969 (ref. 2). In the ESB process glass and metal (or semiconductor) surfaces are placed in contact and heated to a temperature on the order of 300°C to 600°C. A voltage ranging from a few hundred to 2000 volts is then applied so that the glass is negative with respect to the metal. Under these conditions the glass forms a strong, permanent bond to the metal surface. The unique feature of this process is the relatively low temperature at which the bond is made. It is generally 200°C to 400°C below the softening point of the glass.

The application of this process to the formation of integral cover glass solar cell assemblies was first reported in 1975 (ref. 1). The application of the process to integral cover glasses has been of considerable interest for both terrestrial and space purposes (ref. 3). Development of the back surface field enhanced solar cell which permits high efficiencies in thin (2 mil) cells has increased interest in the ESB process. The full exploitation of the potential of thin cells requires thin cover glasses (2 mils is desirable) and for such thin cells and cover glasses, the ESB technique offers significant advantages from the standpoint of reduced weight and ease of fabrication by eliminating the adhesive layer.

The work reported in this document was primarily empirical. The program had three major tasks which were performed in three phases. The first

task involved an investigation of fundamental parameters for bonding glass to AR-coated silicon surfaces. The second task was aimed at extending the investigation to bonding glass to solar cells having a variety of contact grid patterns. The third task was for the production of bonded cells to be delivered to NASA Lewis. An outline of the program tasks is given in table 1-1.

During the first phase of the program (task I) wafers having etched surfaces similar to solar cells but without contact grids were used to determine the effects of varying bonding temperature, T , voltage, V , time, t , pressure, P , and atmosphere. Effects of various glass and wafer variables were also evaluated. These variables included the thickness of Ta_2O_5 AR-coatings, silicon surface texture, and various glass treatments. The glass treatments involved 1) immersion in molten $LiNO_3$ in an attempt to exchange Na^+ ions in the glass for more mobile Li^+ ions and 2) immersion in aqueous solutions of various metallic salts to produce adsorption of the metallic elements into the glass surfaces.

In the second phase of the program (task II) bonding of glass to solar cells with various grid patterns was investigated. To avoid undue thermal degradation of the cells the ESB process had to be restricted to solar cell temperatures below the softening point of the glass. The most significant problem encountered was deforming the glass over the contact grid so that the glass and AR-coated silicon surfaces were close enough to allow the ESB process to progress. Two methods of attacking the problem were investigated.

One method involved heating the glass with a short burst of laser energy using a wavelength such that most of the energy was absorbed in the glass and not the cell. This method showed promise; however, optimization of bonding parameters, hardware configuration, etc., must still be worked out before an entire cell can be successfully bonded using the method.

The other method utilized a bonder cathode material with appropriate compressibility ("cathode pillow") such that the glass over the raised contacts presses into the pillow while the surrounding pillow material bends the glass into the valleys between the contact fingers. The problem is thus turned from one of compressing glass to bending glass. The cathode pillow method has been used to produce many well-bonded samples for the third program phase (task III). Good bonds, however, were achieved only with one of three cell types supplied.

The research and results are discussed in detail in the following sections. Section 2 gives background information on the ESB process, the hardware used in this program, and the parameters monitored during the bonding

process. Section 3 gives physical details of the cover glass, wafers, and cells used in this investigation. These samples were made available by NASA Lewis Research Center. The various aspects of the work performed as indicated in the table of contents and the results obtained on each are discussed in detail in sections 4, 5, and 6. Section 7 summarizes the major conclusions reached. The development of mechanical screening tests and measurements of solar cell electrical parameters before and after bonding were required for this program. The methods developed and used are discussed in appendices A and B. It was also necessary to develop a method for forming notches in the cover glass to facilitate electrical contact. This development is discussed in appendix C.

TABLE 1-1. ELECTROSTATIC BONDING TASK OUTLINE

TASK I ESTABLISH (T, V, t, P) SURFACE USING Ta_2O_5 AR-COATED SILICON WAFERS
INVESTIGATE THE EFFECTS OF:

NITROGEN VERSUS VACUUM

REPLACE Na WITH Li USING LITHIUM NITRATE ION EXCHANGE

ADSORPTION OF METALLIC CATIONS USING AQUEOUS SOLUTIONS OF METAL
SALTS

Ta_2O_5 THICKNESS

TASK II EXTEND PROCEDURES TO BONDING GLASS TO SOLAR CELLS

LASER SOFTENING OF GLASS

CATHODE PILLOW ASSISTED BONDING

TASK III PREPARE SOLAR CELLS FOR NASA LEWIS RESEARCH CENTER

2.0 PROCESS DESCRIPTION AND BONDING APPARATUS

2.1 THEORY

The physics of the processes responsible for the formation of the bond in ESB are not well understood. However, it is generally assumed that the final bond is a chemical bond. This is based on the fact that the bond strength (typically 2000 to 3000 psi) (refs. 1,4) is usually as good as the strength of the glass itself. For chemical bonding of two materials to take place, it is necessary to bring the surfaces within molecular distances of each other. When one material is in a liquid form, this is called wetting. Solid surfaces normally considered to be flat are in fact usually quite irregular on a microscopic scale, and particularly on a molecular scale, so that when two solid surfaces are brought together, they only make contact at relatively few points.

It has been postulated (refs. 1,4) that one role of the electrostatic field in the ESB process is to pull two irregular surfaces into the intimate contact required to form a chemical bond. Most glasses contain mobile positive ions compensated by almost immobile negative ions. Considering such a material sandwiched between two electrodes which are not sources for mobile positive ions, the positive ions in the glass would be pulled away from their respective anions toward the cathode. This is depicted in figure 2-1 which illustrates some aspects of the ESB process. Since electrons are available from the electrodes, they will move into the glass to combine with the displaced positive ions causing a net negative charge in the glass. Thus, the glass will be attracted to the positive anode with an electrostatic force. It was hypothesized that a negative space charge occurs initially over a thin glass region near the anode and widens as time progresses. For a given degree of polarization and space charge, the attraction between the glass and anode will be largest where the spacing is minimal. As the space charge grows with time, the glass and anode are pulled together from the gap edges and the field strength in the gaps becomes larger so that initially wider gap areas are pulled together. Thus, intimate contact and bonding would progress outwardly with time from the initial points of contact consistent with observations of the ESB process. In this process an electrostatic attraction of 350 psi has been measured between Pyrex and a metal anode (with "zero" gap at 300°C, and 800 volts) under conditions which did not produce bonding (refs. 1,4).

CRITICAL PARAMETERS

PRESSURE P
VOLTAGE V
TEMPERATURE T
TIME t

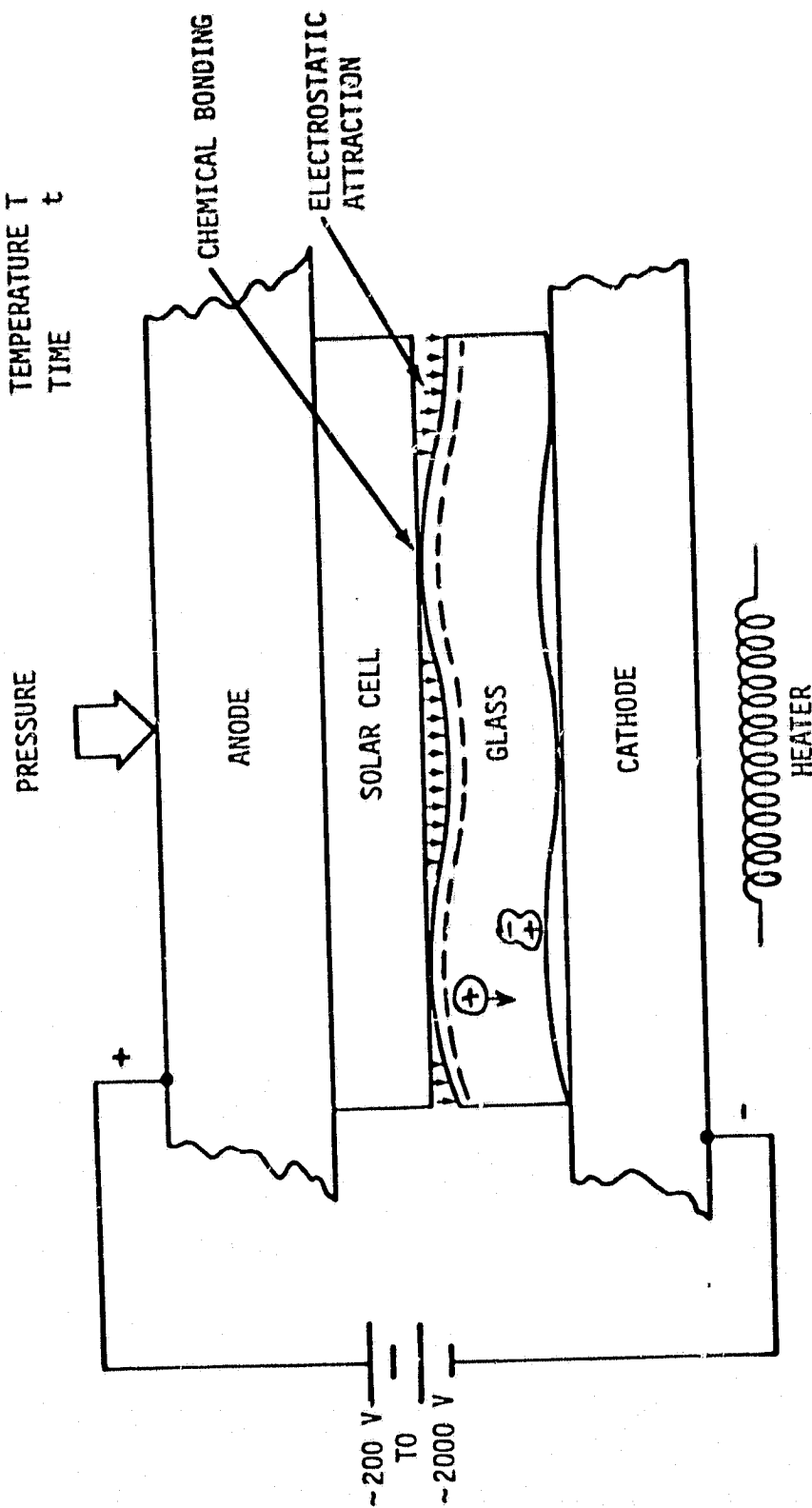


Figure 2-1. Schematic Showing Aspects of Electrostatic Bonding

2.2 BONDING APPARATUS AND BASIC PROCEDURE

The important aspects of the apparatus (bonder) used to make electrostatic bonds in this investigation are depicted in figure 2-2. A photograph of the bonder is shown in figure 2-3.

In the bonding runs, the glass was laid on the cathode heater (C/H block) and the cell was laid front side down on the glass. After the bell jar was evacuated, power was applied to heating coils in the C/H block to heat the cathode and glass. The cathode temperature was monitored using a thermocouple at the point indicated in figure 2-2. When the cathode temperature reached the desired value, the desired pressure was applied uniformly over the sample surfaces by raising the gas pressure in the anode bellows to an appropriate level. The cathode and anode surfaces were machined to close tolerances to apply uniform pressure over the entire sample area. The anode temperature was also monitored with a thermocouple at the point indicated on figure 2-2. Whenever a temperature is given without qualification, it is understood to be the anode temperature averaged over the time of bonding. When the anode temperature reached a value which indicated that the sample had been heated to the desired temperature, the bonding voltage was applied from anode to cathode and bonding proceeded. When the bonding interval was over, gas pressure was applied to the cooling bellows so that the cooling block contacted the C/H block and cooled the sample. When the temperature of the cathode dropped to a level at which it would not oxidize ($\lesssim 100^{\circ}\text{C}$), the bell jar was brought to atmosphere and the sample was removed.

The bonder was constructed to facilitate a one sample at a time research effort with the possibility of varying and monitoring important bonding parameters. A block/functional diagram of the controlling electronics and data monitoring system is shown in figure 2-4. On each bond run, the C/H block temperature, anode temperature, applied voltage, sample current, and time integral of sample current were recorded as a function of time using strip chart recorders.

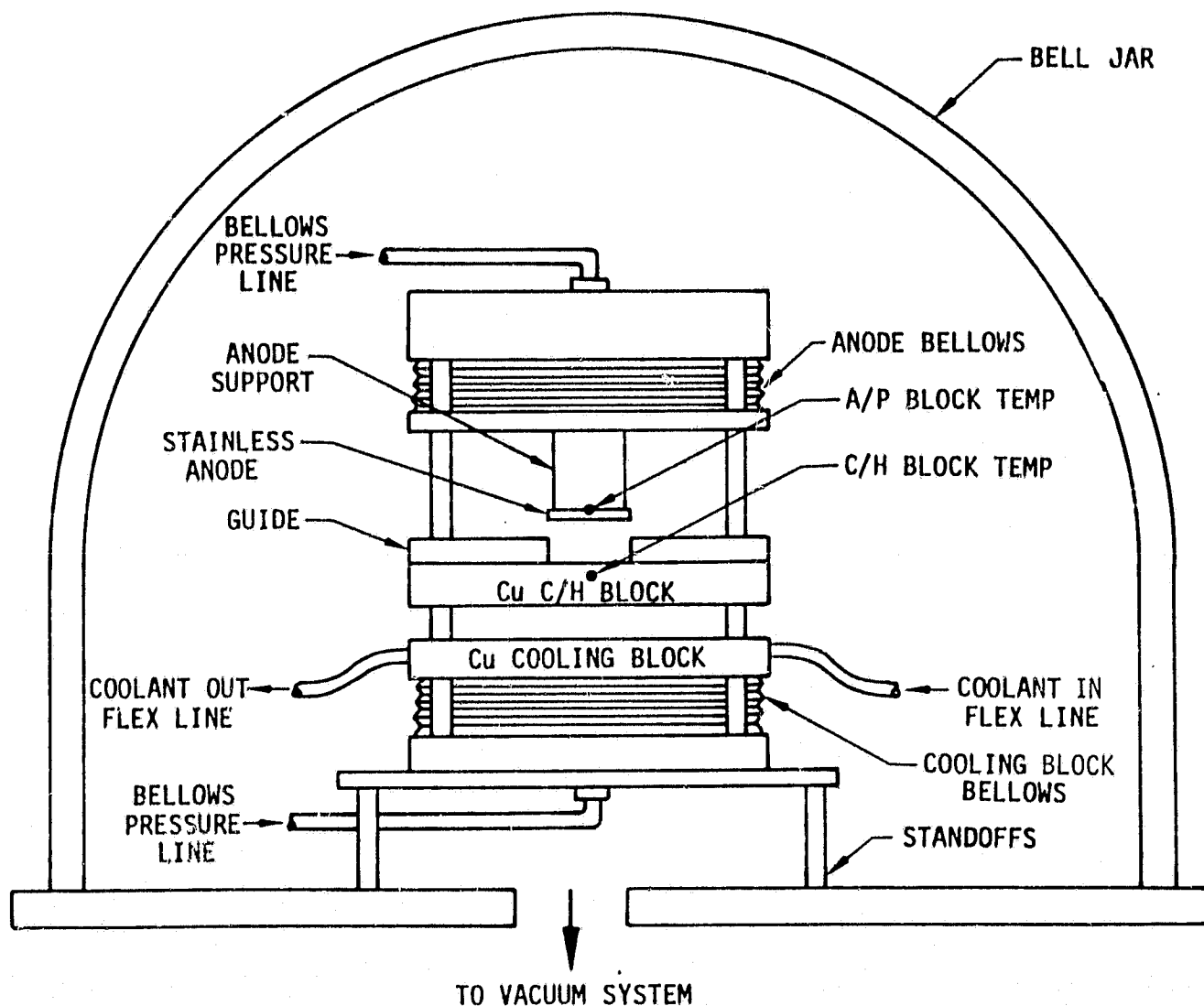


Figure 2-2. Conceptual Drawing of Bonder Head

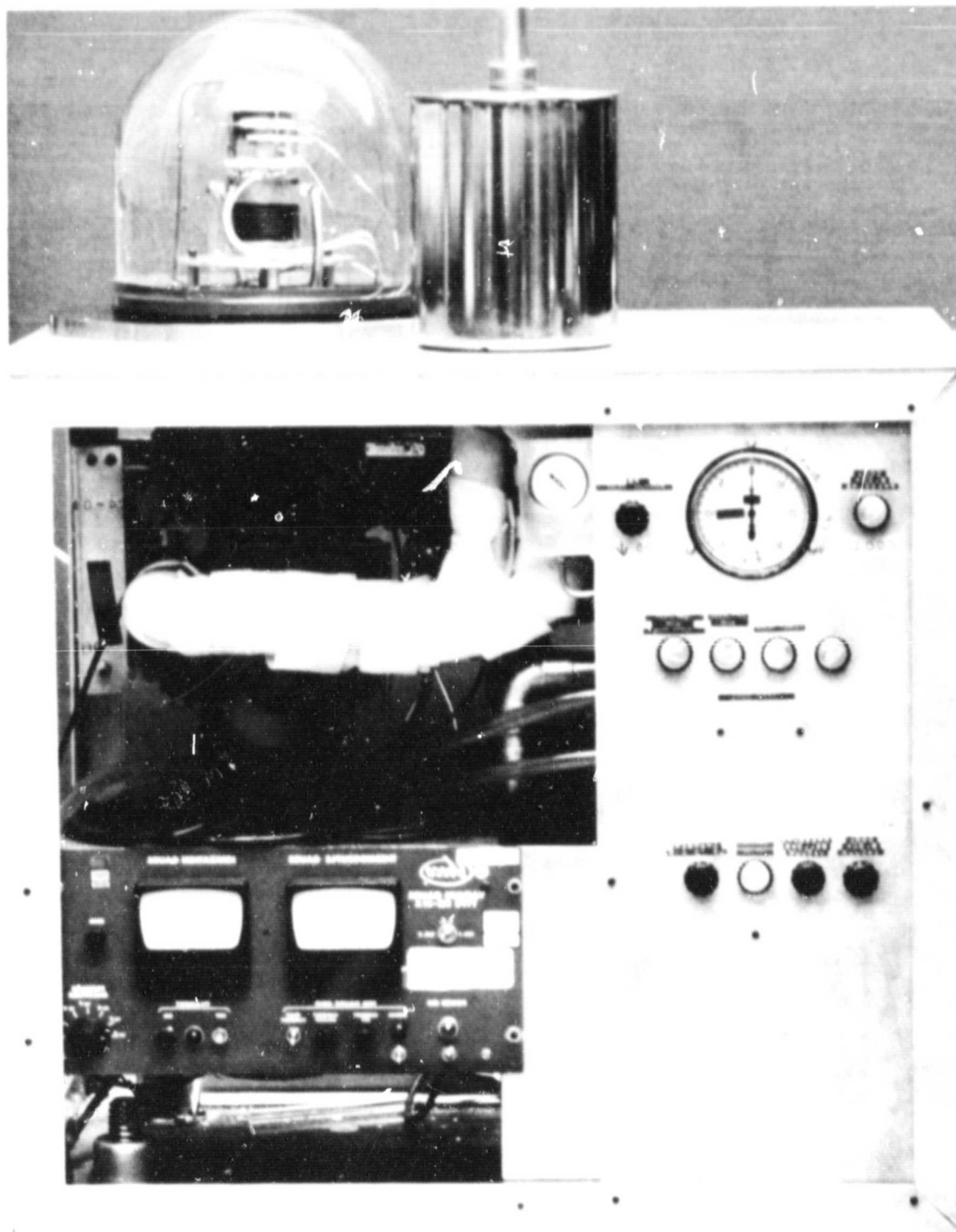
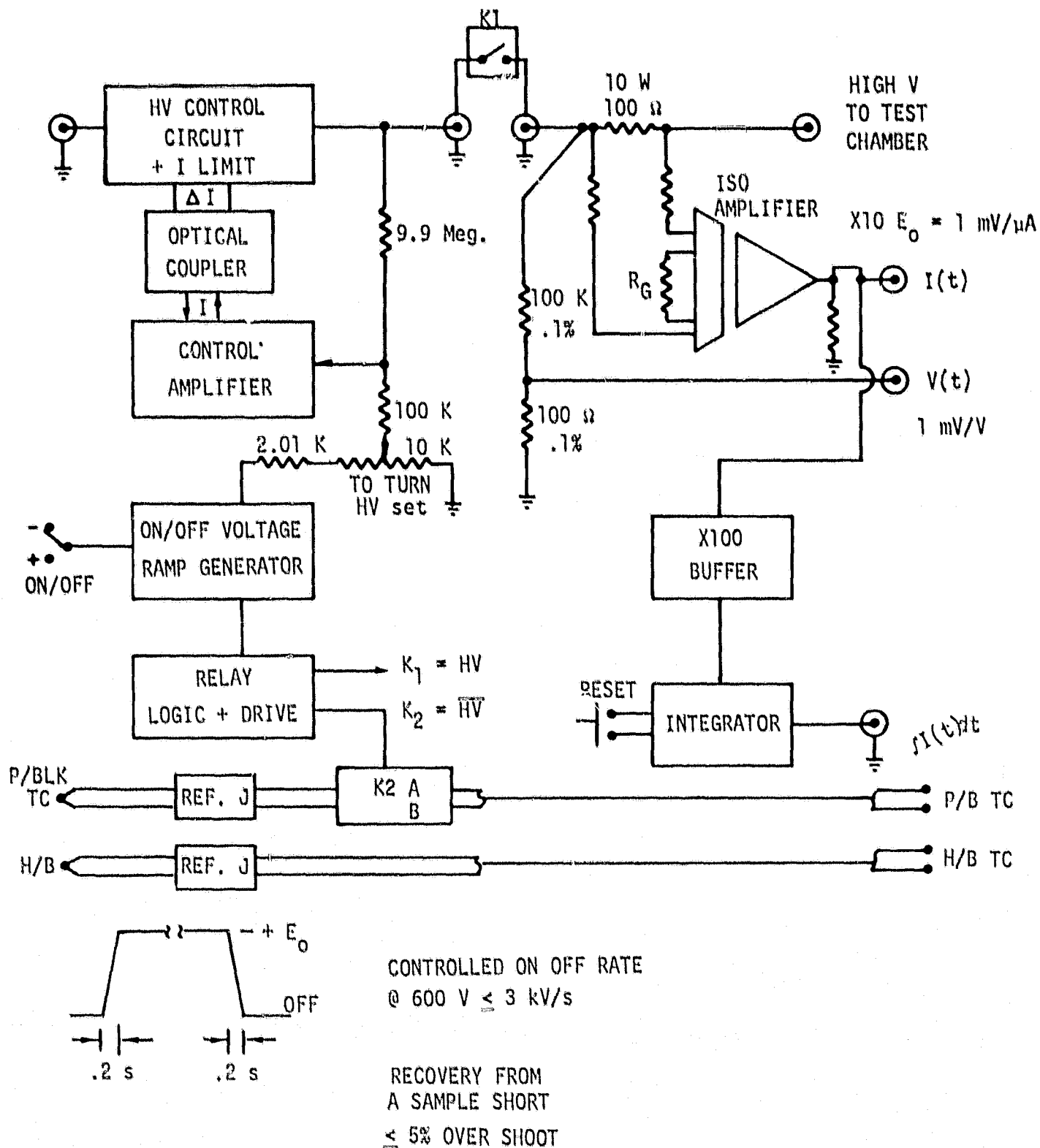


Figure 2-3. Photograph of ESB Bonder



E_0 DIAL SET $100 + 800 \text{ V}$ WITH $E_{in} \approx 50 - 100 \text{ V}$ GREATER THAN E_0 SET

Figure 2-4. Bonder Control and Data Acquisition System

3.0 SAMPLE DESCRIPTIONS

3.1 COVER GLASS DESCRIPTIONS

The Corning 7070 cover glasses were supplied in three lots. The reported composition of 7070 glass is given in (ref. 5). The dimensions of the samples were approximately 2 cm by 2 cm by 3 mil. Significant variations in thickness occurred. The thicknesses were measured on five random samples from each lot. The results are given in table 3-1.

Table 3-1: SUMMARY OF GLASS THICKNESS MEASUREMENTS
(5 Samples Each Lot)
(\bar{x} = mean, s = sample standard deviation)

Lot I, \bar{x} = 3.5 mil and s = 0.13 \bar{x} ;
Lot II, \bar{x} = 2.7 mil and s = 0.01 \bar{x} ;
Lot III, \bar{x} = 2.8 mil and s = 0.08 \bar{x} .

All lots contained a large fraction of glasses with considerable surface irregularity (striations and bubbles). However, lots II and III, were markedly better than lot I in this regard. A typical striation profile for lot I is shown in figure 3-1(a) which was produced by a Taylor Hobson Talysurf IV (an instrument which mechanically tracks the surface profile by dragging a micro sharp needle over the surface). It is believed, that such striations indicate a variation in the process for forming the thin glass microsheets, which would likely result in variations in glass composition from sample to sample. Considerable variations in the amplitude of bonding current from sample to sample were observed under otherwise near identical conditions. For example, nine samples were bonded using the same conditions of T , V , t and P . The resultant differences in average bonding current ranged over an order of magnitude. This is probably due in large part to glass composition variations.

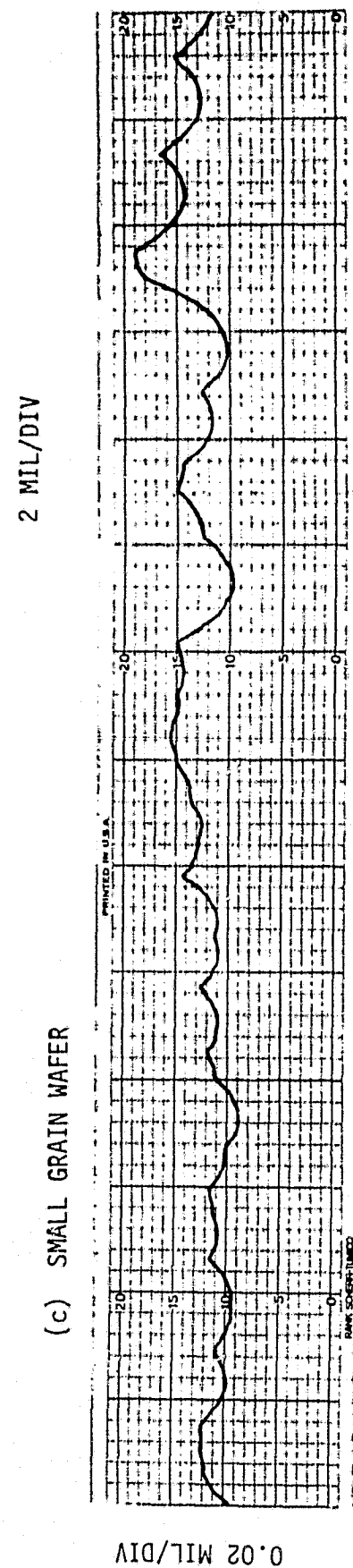
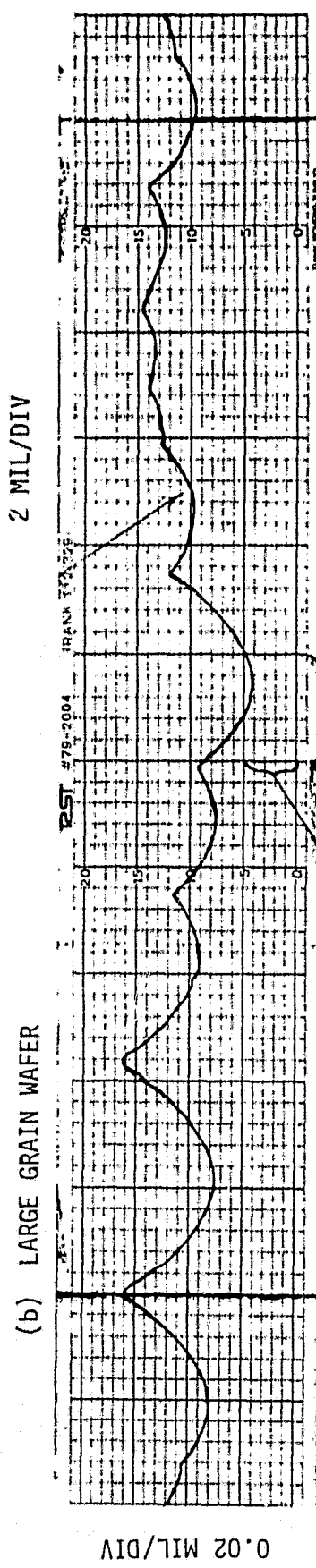
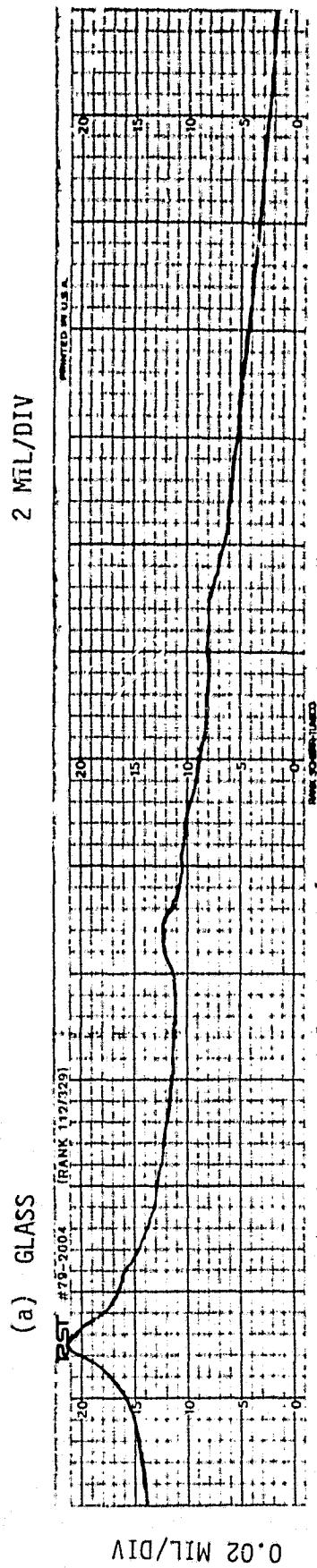


Figure 3-1. Wafer and Glass Surface Profiles

3.2 SILICON WAFER DESCRIPTIONS

The silicon wafers which were available for this research were about 2 cm by 2 cm by 3 mil. The surfaces were etched and coated on one side with a Ta_2O_5 layer to simulate the surface of typical solar cells of interest. The thickness of the Ta_2O_5 layer is not known, however the color of the layers indicates that it is likely in the range of about 600 Å to 800 Å. The etched surface topography consists of rounded bottom pits of various sizes separated by relatively sharp ridges. As the program progressed, it was discovered that the available wafers could be put roughly into two categories, "large grain" and "small grain," based on microscopic examination of typical pit size. Example tally graphs showing cross sections of the surface profiles were shown in figure 3-1 b and c. A photograph of a typical wafer surface is shown in figure 3-2a. Figure 3-2b shows such a wafer with glass bonded. The deepest pits are visible as light regions due to incomplete bonding as discussed later in section 5.1.2.

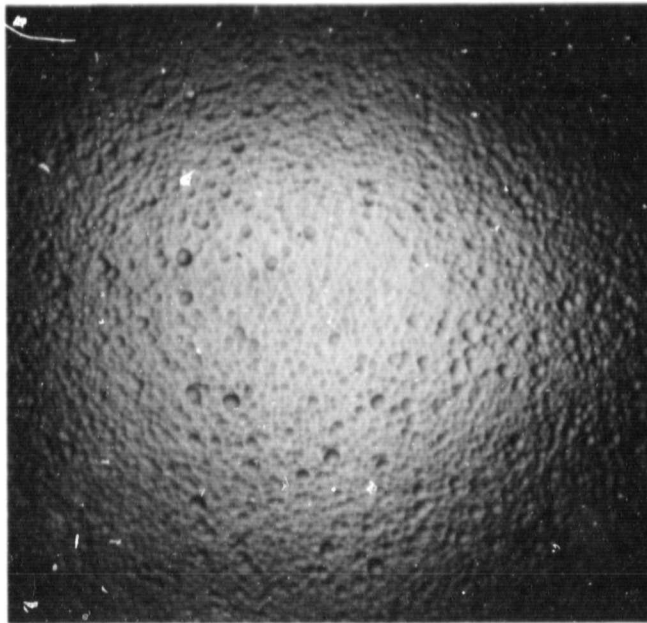
The above described wafers were used for most task I investigations except as noted. The major exception was the evaluation of Ta_2O_5 thickness effects. For this effort, smooth nonetched wafers were coated at NASA with the following thicknesses of Ta_2O_5 : 385 Å, 431 Å, 570 Å, 610 Å, 660 Å and 760 Å.

3.3 SOLAR CELL DESCRIPTIONS

Three types of solar cells were used in this investigation. They are identified by the three grid patterns as shown in figure 3-3. The cells are referred to as herringbone, rectangular and bar grid. The thicknesses were respectively √3 mil, √2 mil, and √3 mil. The surface finish of the herringbone and rectangular grid samples was similar to the wafers described above. The bar grid samples, however, had a surface which was much finer in structure. The surface appeared texturized at magnifications similar to figure 3-2 but had a sharp, random, crystalline appearance at much higher magnifications of 450x.

Tallysurf profiles showing the surface textures and relative contact height and separation are shown in figure 3-4. The location of the contact paths is indicated by arrows. It is not clear whether the Tallysurf was able to accurately follow the structure of the bar samples (figure 3-4 c and d) since

(a) BARE WAFER



(b) WAFER WITH GLASS BONDED

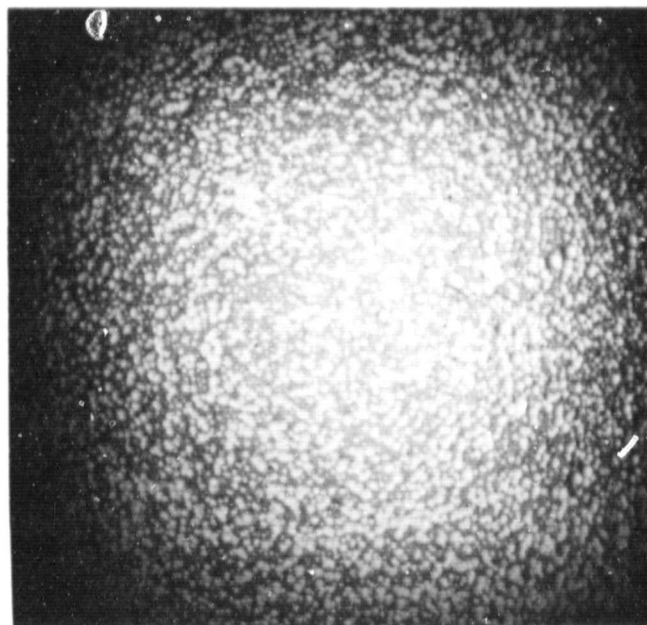
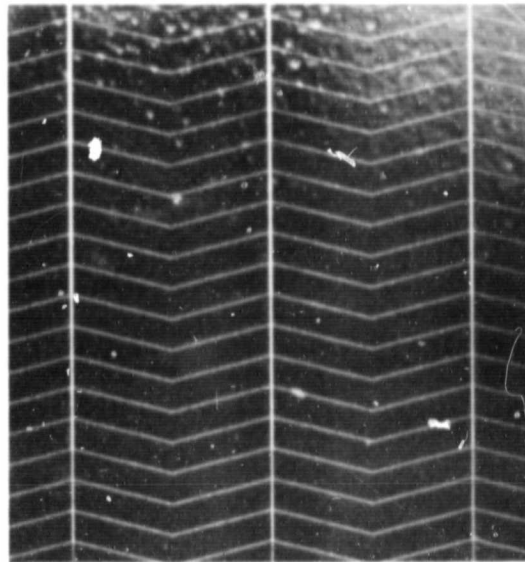
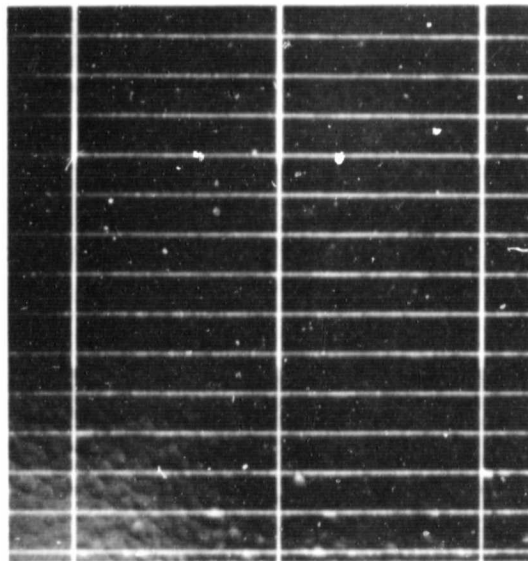


Figure 3-2. Example Photographs of Wafer Surfaces

HERRINGBONE



RECTANGULAR



BAR

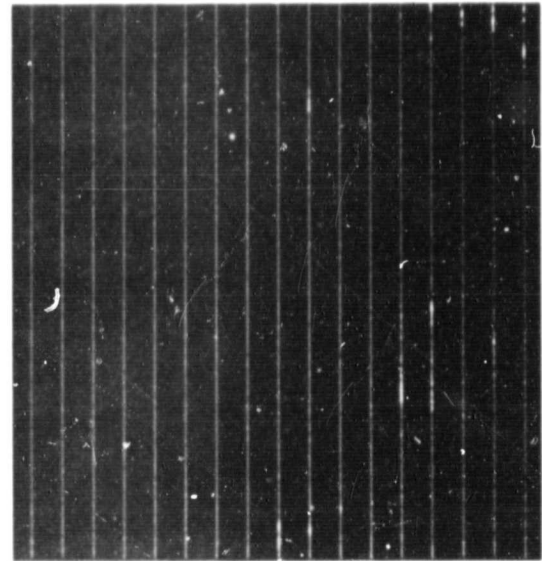


Figure 3-3. Solar Cell Grid Patterns

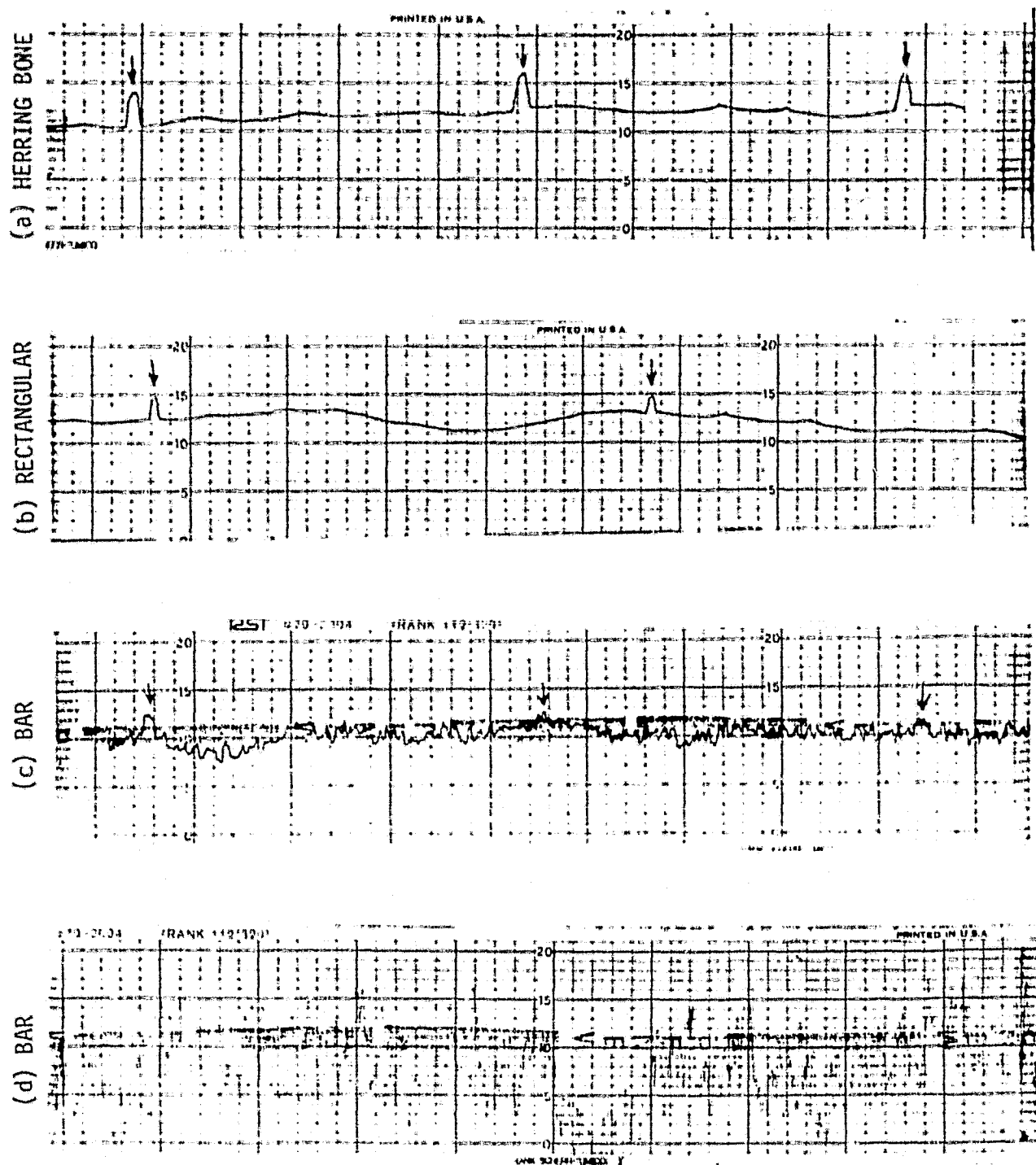


Figure 3-4. Example Surface Profiles of Solar Cells

(Scale for a, b, and c: Vertical = 100 μ inch/div; horizontal = 2 mil/div).
 (Scale for d: Vertical = 20 μ inch/div; horizontal = 2 mil/div).

the higher magnification shown in figure 3-4d indicates more structure than figure 3-4c. Regardless of the accuracy, the surface is shown to be extremely jagged.

4.0 GLASS PREPARATIONS

4.1 INITIAL CLEANING

The cover glasses were received with considerable debris on the surfaces (glass chips) apparently from the cutting process. These chips were generally too small to be seen with the naked eye prior to bonding, but were quite visible at 100 power with an optical microscope using direct-through-the-lens lighting. Since the debris affected the quality of the end product significantly, a method of cleaning had to be developed.

Ultrasonic baths were tried using solutions such as alcohol and also a detergent solution (7-x from Linbro Scientific Inc. Hamden Ct.). These methods would not remove the chips. The most successful method found was: 1) hold the glass samples on a vacuum chuck and scrub them with 7-x detergent using a soft toothbrush, 2) rinse the samples in distilled H_2O , and 3) dry the samples in a warm ultrapure nitrogen blast or vacuum oven.

On the first lot of cover glasses which were nominally 3.5-mil thick this procedure was quite easy. Tweezers were used to handle the glasses and they were blown dry between a dual nozzle arrangement which equalized the nitrogen blast on both sides of the glass. Lot II samples (\sim 2.7-mil nominal thickness) were extremely difficult to handle without breaking. Drying was facilitated by placing the samples in a quartz rack in a vacuum oven at \sim 150°C. Lot III samples were much less fragile although the nominal thickness was close to that of lot II. This may indicate a further difference in the glass composition.

4.2 FORMATION OF NOTCHES IN COVER GLASSES

In order to obtain maximum protection by the cover glass from space radiation environments, it is desirable to cover the maximum area of the solar cells leaving a minimum uncovered area to make electrical contacts. Since the cover glasses and cells were both 2 cm by 2 cm, it was necessary to develop a means of making notches for the areas of the solar cells to be electrically contacted. Several methods were tried before a satisfactory solution was found. The method which was successfully employed is discussed below. (The other methods investigated are described in appendix C.)

Notches were cut in the glass with a diamond saw. A milling machine was used with the glass clamped in stacks between the jaws of a special vise. The vise was fabricated to hold stacks of glass samples with pressure only at their periphery. In the first attempt, vise jaws were used which covered the full glass area. An unacceptable breakage problem occurred as a result of nonuniform stress caused by clamping the samples over bubbles in the glass. Usually when a piece of glass with a bubble was included in the stack, the entire stack would break. Since about half of the samples had at least one bubble, this was unacceptable. The problem was eliminated by relieving the vise jaws so they applied pressure to the glass samples only around their periphery. Due to the reduced-contact area, enough samples were available without bubbles in the pressure region so that such samples could be used exclusively and the breakage problem was eliminated.

5.0 TASK I - BONDING GLASS TO SILICON WAFERS

5.1 PRELIMINARY PROCEDURE DEVELOPMENT

Before the primary objectives of task I could be pursued, a number of unanticipated problems had to be worked out. The problems of most interest are discussed in this section.

5.1.1 Glass Damage

Preliminary set-up and check-out of bonding procedures were made using polished bare silicon wafers. The initial bonder cathode surface was machined copper. Although complete bonds were easily accomplished, considerable glass damage occurred. Some typical examples are discussed below.

One glass effect is shown in the photograph of figure 5-1. Many possible causes were questioned, including phase separation in the glass. However, observations indicated, that the damage was related to the microscopic surface finish of the cathode and perhaps a reaction between the copper and the glass. Other materials such as stainless steel and gold were tried with unsatisfactory results.

It was postulated that tantalum would not react as readily with the glass and thus a Ta foil overlay was tried. This worked fairly well, except for a high density of point defects. These are shown in figure 5-2a as black dots and one of these is shown at high magnification in figure 5-2b. The appearance of this damage stimulates the hypothesis that it is associated with some sort of electrical point discharge accompanied by high heat. It was speculated that electrical discharges might have occurred at high points on the cathode surface leading to the observed damage. A Ta cathode overlay was then lapped and polished to a micro mirror finish using a 1.0 micron grit polishing compound. Initial bonds made with this surface showed no damage. However, the problem sporadically cropped up again later. A polished silicon wafer was tried for a cathode surface in the belief that this would provide the ultimate in surface finish. These surfaces are completely mirror like with no surface structure visible even at $\times 1000$ magnification. Point damage to the glass still occurred although it was slightly different in microscopic structure. Also, unlike the other cathode surfaces used, a rather exotic damage pattern occurred on the

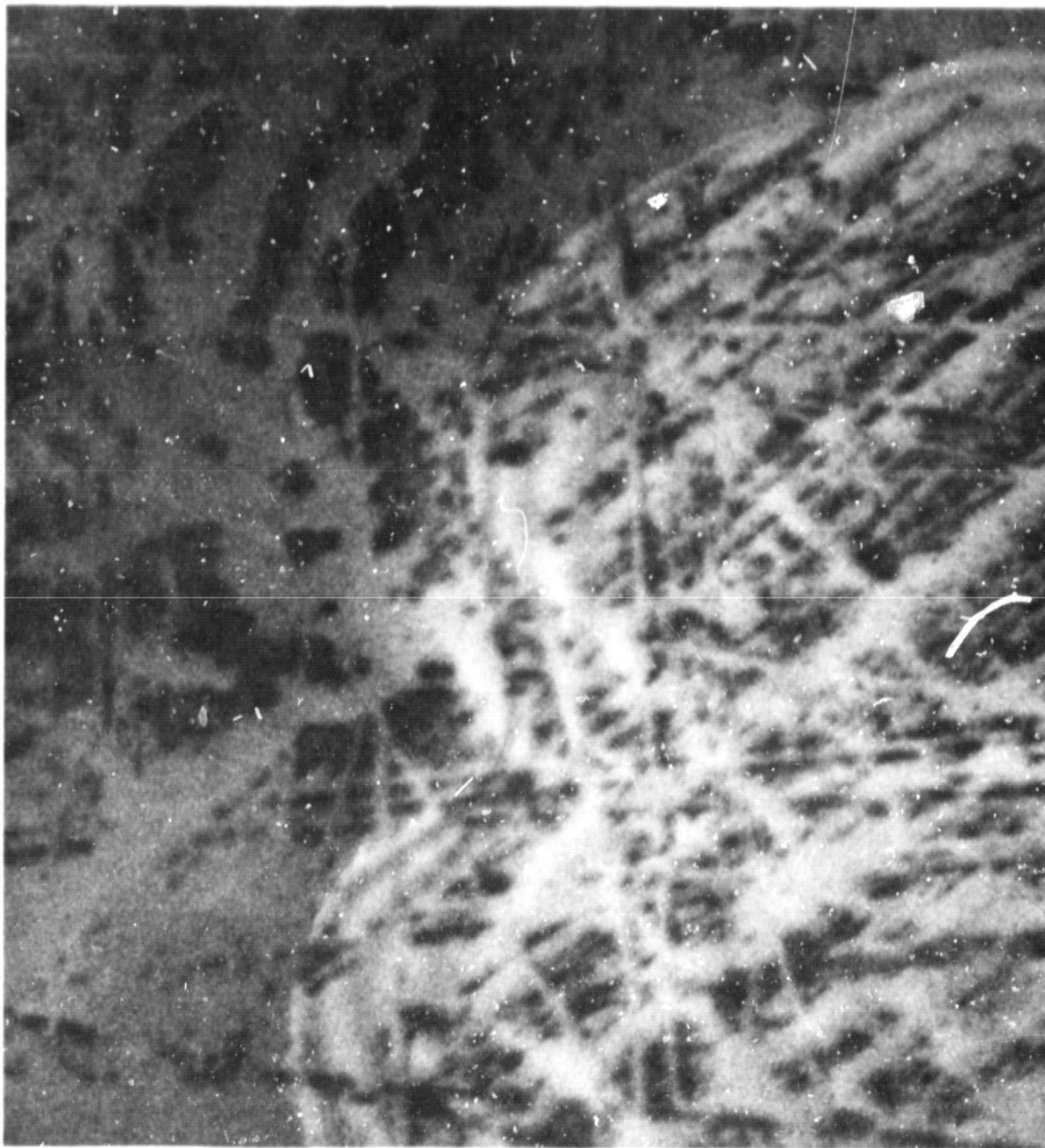
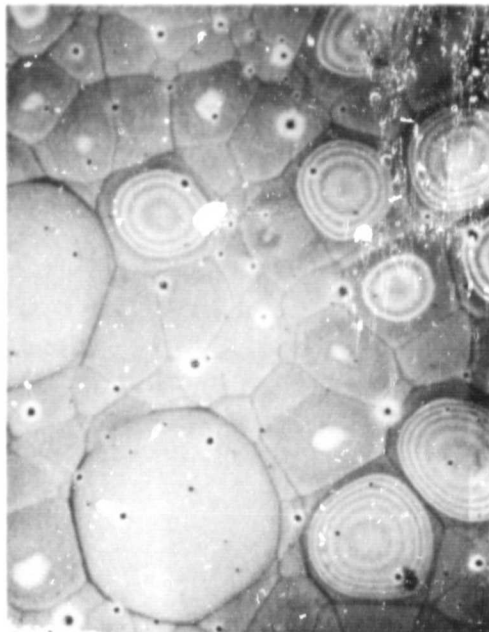


Figure 5-1. Glass Damage Observed Using Machined Copper Cathode

ORIGINAL PAGE IS
OF POOR QUALITY

(a) AND (b) GLASS DAMAGE RESULTING WITH UNPOLISHED Ta CATHODE

(a) Relative Magnification = 50X



(b) Relative Magnification = 450X



(c) DAMAGE TO POLISHED Si CATHODE ASSOCIATED WITH GLASS DAMAGE
SIMILAR TO THAT SHOWN ABOVE

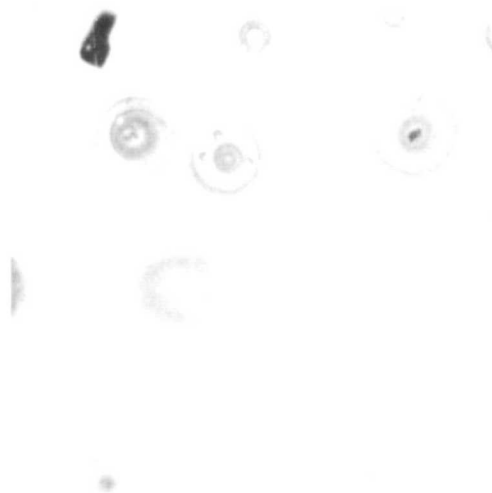


Figure 5-2. Examples of Glass and Cathode Damage Due to Hypothesized Discharge

silicon cathode surface. An example is shown in figure 5-2c. Because of the need to press on with the primary objectives of the program, further investigation of this problem was not pursued. Although the problem occurred somewhat sporadically throughout task I, it was not observed with the soft cathode pillow developed and used in tasks II and III and discussed later in section 6.3

5.1.2 Determination of Degree of Bonding

Bonding to etched silicon was found to be considerably more difficult than bonding to polished silicon. Due to the irregular surfaces, bonding is microscopically very irregular as can be seen in the photomicrograph of a bonded sample shown in figure 5-3. The interference fringes indicate air gaps on the order of a micron between the glass and semiconductor surface. It was initially not clear which regions were bonded and which were not. Some observers hypothesized that bonding had occurred only at the center of the circular fringed regions. However, based on the surface structure of the samples as discussed in section 3.2, it seemed most likely that bonding would be initiated at the sharp peaks and ridges and then progress out into the rounded pits. Considering the relative position of the interference fringe boundaries and the pit boundaries this would be consistent with the conclusion that the regions showing no interference fringes are bonded and those showing fringes are unbonded. This conclusion is also consistent with the fact that the fringes are sharper and more closely spaced at the outer edges of the fringed region versus the central regions. A proof that the fringed regions are unbonded while the regions without fringes are in intimate contact (and thus must be bonded considering the surface irregularity) was obtained by applying pressure with a sharp pin while observing the pattern through a microscope. When pressure is applied in the fringed regions, the fringes move in toward the center and the areas of the fringed regions shrink. When pressure is applied in the regions adjacent to the periphery of the fringed regions, no changes occur.

The next problem was to define the percentage of bonding and set criteria for acceptable and unacceptable bonds. Peel and temperature cycling screening tests were developed as described in appendix A. Regions containing about 30 percent or more microscopic bond coverage withstood both peel tests and temperature cycling. However, if any significant macroscopic region was bonded

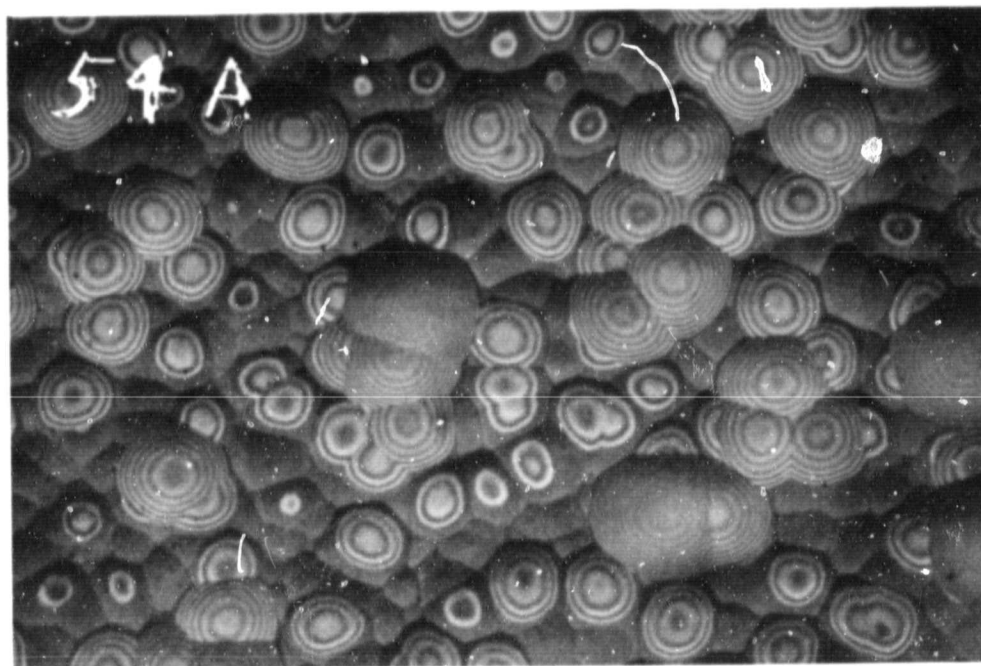


Figure 5-3. Example Photomicrograph of Wafer With Glass Bonded

ORIGINAL PAGE IS
OF POOR QUALITY

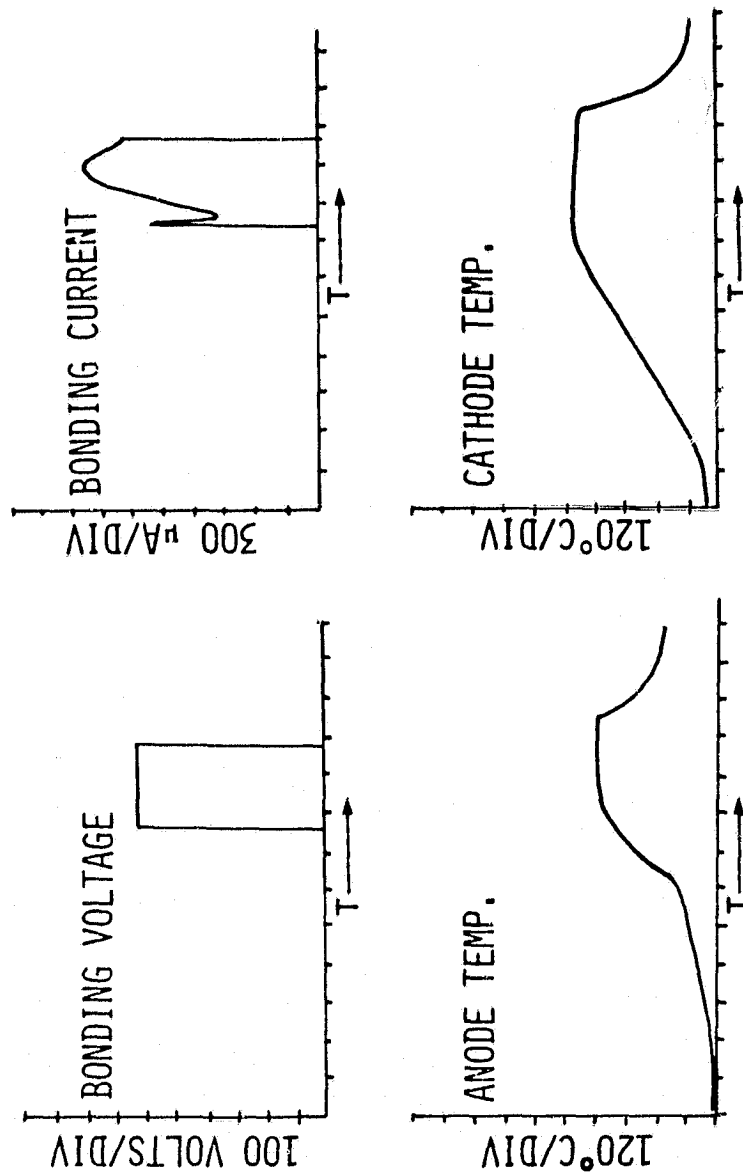
much less than this, the glass in that region would cling to the tape and break away generally leaving the bonded regions unaffected. It was decided that roughly ≥ 50 percent bonding on a microscopic scale and ≥ 95 percent bonding on a macroscopic scale would constitute a good bond.

The next problem was to find a means of readily determining the degree of microscopic bonding over the entire area of a 2 cm by 2 cm sample. Since somewhat subjective judgments had to be made, a means was needed of viewing more than one entire sample at a time and comparing samples with high enough magnification to judge the microscopic degree of bonding. A photographic technique was developed to provide photographs like that shown in figure 3-2b. The dark regions were correlated to bonding and the light regions correlated to no bonding. It was necessary to use a large uniform source of parallel light and illuminate the sample through a 45-degree beam splitter over the sample to provide the required visual effects which would differentiate between bonded and unbonded regions. Such photographs coupled with microscopic spot examination of each sample were used to facilitate the judgment of bond quality. The photographs shown in figures 3-2b and 5-3 illustrate roughly the degree of bonding considered to be ≥ 50 percent on a microscopic scale and ≥ 95 percent on a macroscopic scale.

5.1.3 Bonding Parameters and Bonding Approach

The initial test plan called for finding the optimum values of bonding voltage, V, pressure, P, time, t, and temperature, T by an iterative procedure starting at some intermediate set of (P, V, t, T) below the maximums of P = 55 psi, V = 800 volts, t = 10 minutes, and T = 550°C and changing at least one parameter on each test sample. Using such a procedure, it should be possible to define a surface in the four dimensional (P, V, t, T) space which separates parameter sets that yield good bonds from those which do not. This of course assumes that all samples are identical and that enough samples are available to define the surface to the degree of detail desired.

Measurement and control of bonding pressure, voltage, and time presented no problem. However, the temperature was something of a problem both to measure and control. First, the temperature of the glass had to be surmised from the temperatures of the bonder cathode and anode measured as discussed in section 2.0. Example profiles of bonding parameters are shown in figure 5-4.



(TIME SCALE, τ , 1 MINUTE/DIV)

Figure 5-4. Example Strip Chart Records of Bonding Parameters

Bond runs were made using 4 mil flat thermocouple leads sandwiched between lot I 7070 glass and a polished Si wafer. Based on these runs, it is believed that the cell temperatures were within a factor of 1.2 of the anode temperatures.

Initially, attempts were made to set the temperature by varying the cathode temperature and letting the anode temperature come to equilibrium. This was found to be very time consuming. Also, different sample sets had considerably different rates of heat transfer so that the difference between the cathode and anode temperatures at equilibrium varied from sample to sample. It is hypothesized that this is due to differences in sample surface smoothness and the resultant thermal transfer area. As a consequence of these problems, as the program progressed, the cathode was raised to its equilibrium value at somewhat higher temperatures than the final desired sample temperature and the bonding voltage was applied at a particular value of anode temperature. The anode temperature would then generally increase during the run and the results were analyzed in terms of the mean anode temperature during the time that the bonding voltage was applied.

The investigation to define the (P, V, t, T) surface was begun using the approach of trying to hit particular points in the four-dimensional space with each sample. However, it was soon discovered that sample to sample variations were so large (up to an order of magnitude in bonding current under identical conditions) that such an approach would not yield meaningful results. It was noted that the average current on one sample, which bonded, was about 230 μ A while that on the second sample, run at similar conditions and which did not bond, was only about 10 μ A. This led to an investigation of sample-to-sample variations and the role of current in the bonding process.

Sample variations were discussed in sections 3.1 and 3.2. It was concluded that since considerable variation existed in both glasses and wafers, (about one order of magnitude in average current out of nine samples bonded under the same conditions) a statistical approach to defining each point on the (P, V, t, T) surface was called for. Unfortunately, enough samples and time were not available in the program to take such an approach without other compromises.

One compromise taken was to limit the variations in pressure. It was speculated that for the silicon wafers used in task I, increasing pressure within the range allowed (≤ 55 psi) would probably be beneficial only up to the point where gross irregularities in the glass could be flattened out. As

discussed in section 2.0, the attractive force per unit area due to the electrical field should be much greater (~ 350 psi at close spacing) so that the effects of mechanical pressure of ≤ 55 psi would be negligible after initial glass flattening. A pressure of ~ 15 psi appeared, based on heat transfer, to be a reasonable value to accomplish initial flattening and was used for subsequent testing.

Considering the large sample-to-sample variations that were present, it was hypothesized that there might be a more direct correlation between $\int I(t)dt$ and the degree of bonding than between time and bonding given the same values of P, V and T. Therefore a circuit was designed and fabricated to give a voltage which was proportional to $\int_0^t I(t)dt$. This voltage was recorded on a strip chart for each run and used to determine how long each bond run should last.

5.2 (T, V, t,) SURFACE DETERMINATION

The results of the investigation of varying T, V, and t with P = 15 psi are summarized in figure 5-5. The data bars roughly indicate the bounds that were established on the transition region between good and bad bonds as defined in section 5.1.2. The precise shape and extent of the surface remains a matter of some speculation; however, the shape shown seems reasonable considering the physics involved and the limited data obtained.

The data were taken by working in the three planes defined by V = 800 volts, V = 200 volts, and t = 10 minutes. Each datum obtained is represented in the planar plots of figure 5-6. The symbol, \vee , means that the temperature required to obtain a "good" bond at the corresponding abscissa value is less than the corresponding ordinate value and the symbol, \wedge , means that it is greater than that value.

A scatter plot of the microscopic percentage of bonding versus $\int I(t)dt$ is shown in figure 5-7. The significant fact is that a good bond was always obtained above a given value of $\int I(t)dt$, regardless of the other conditions. These data indicate that this integral would be a valuable tool; much better than time in determining how long each sample should be bonded, particularly given samples with significant variation in factors affecting bonding current.

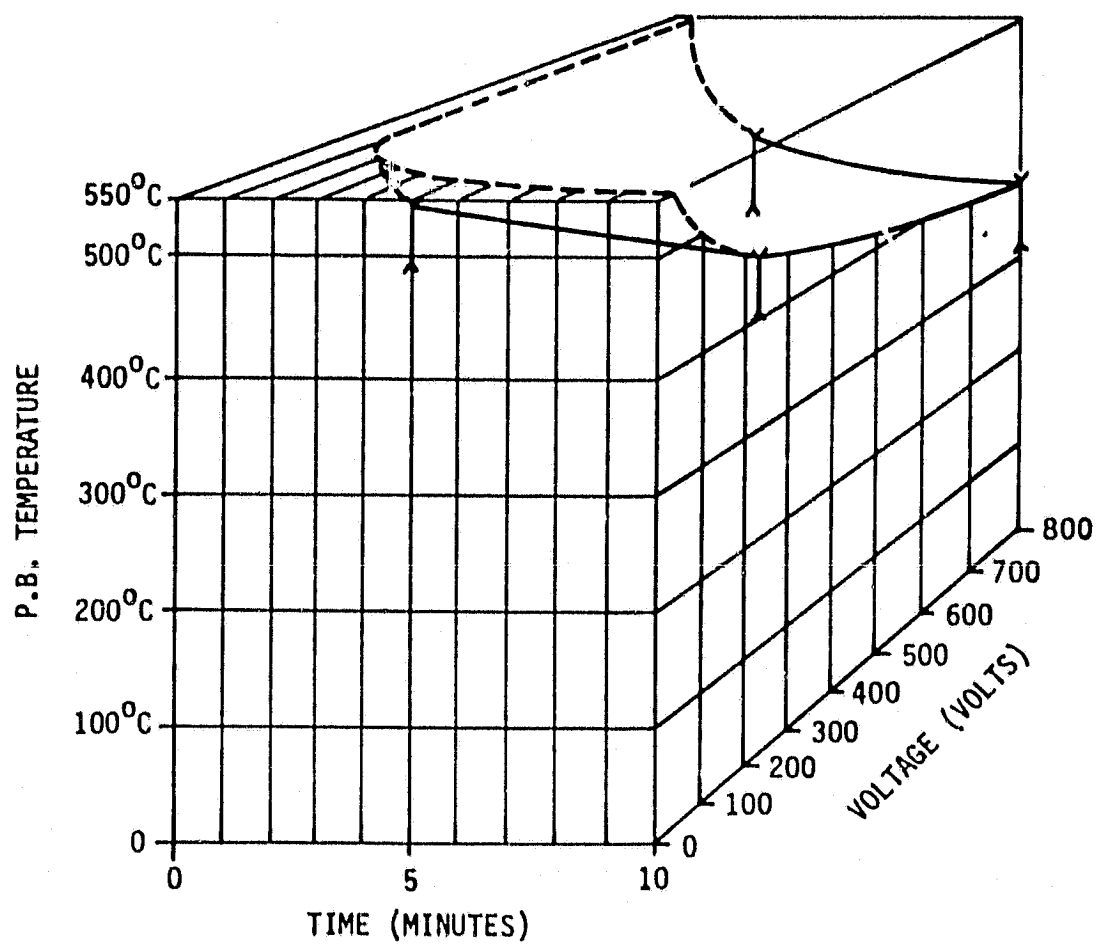


Figure 5-5. Electrostatic Bonding T, V, t Surface

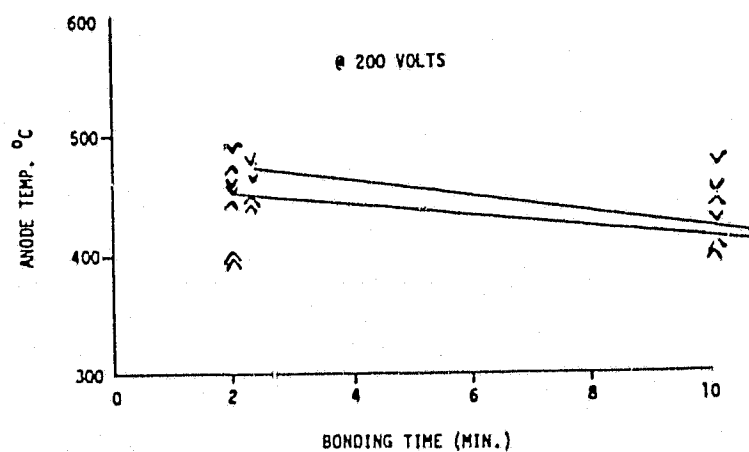
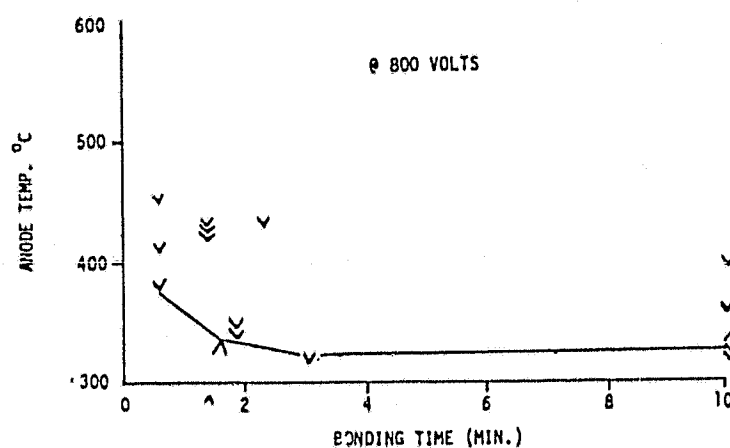
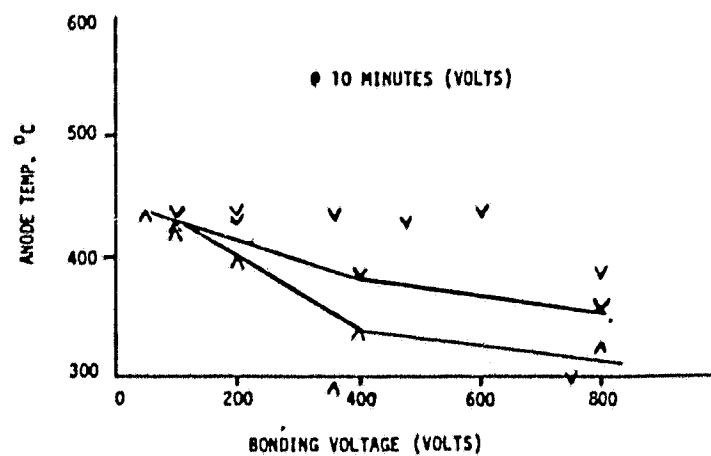


Figure 5-6. Two-Dimensional Plots of Bonding Parameter Dependences for Wafers (^ Bad Bond, v Good Bond)

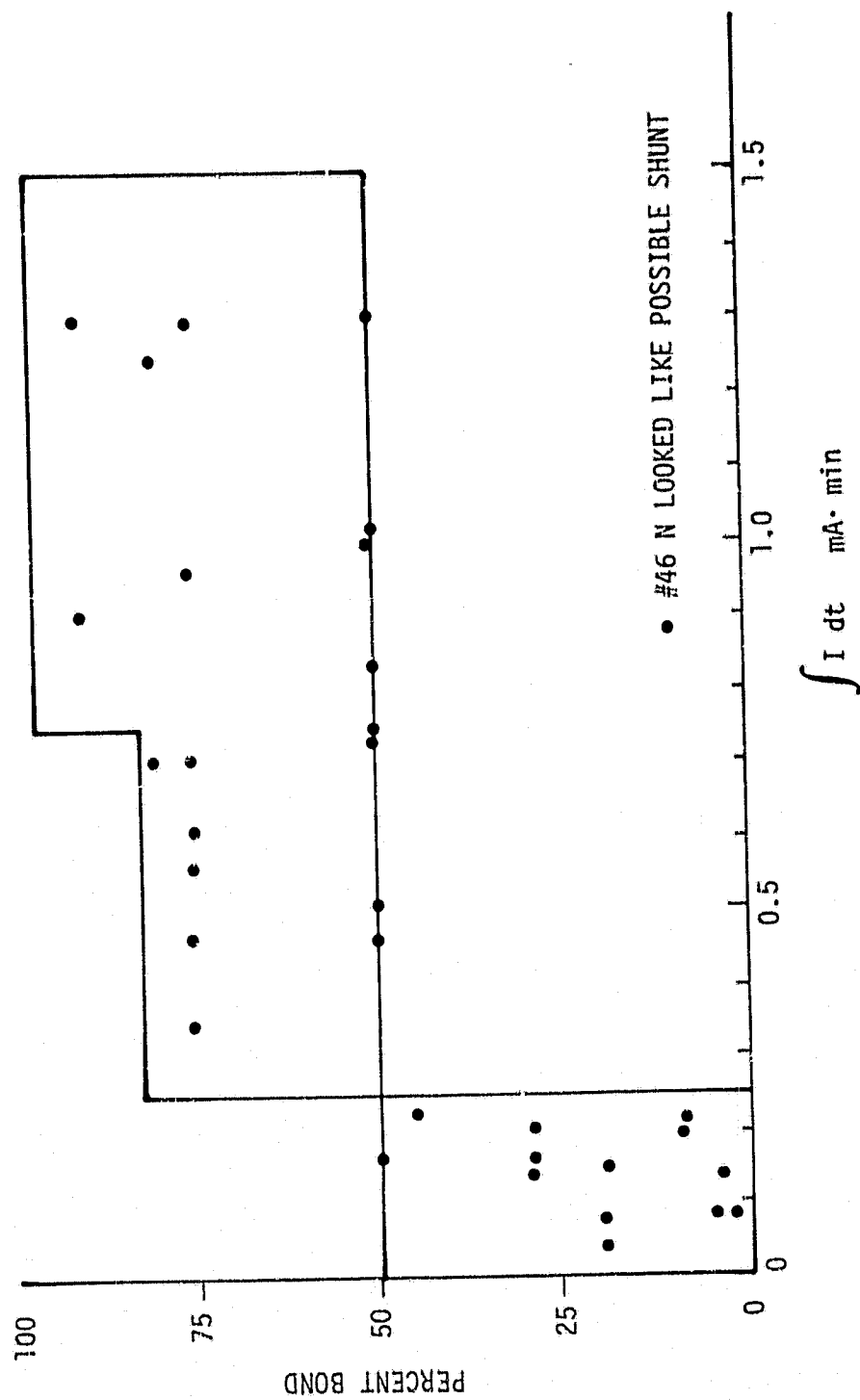


Figure 5-7. Microscopic Percentage Bond Versus $\int I(t)dt$

5.3 AMBIENT EFFECTS

Most of the data for task I were taken in a vacuum obtained by pumping the bonding chamber from the room atmosphere down to pressures between 10^{-4} Torr and 2×10^{-4} Torr. Although the bonder was equipped with a diffusion pump, lower pressures were not tried for task I since it was felt that other problems were of greater importance. The primary effects of the ambient atmosphere are believed to be heat transfer, oxidation of bonder components, and maximum applicable bonding voltage.

With the vacuums used, oxidation of bonder components at the temperatures employed was essentially eliminated and the maximum voltage for this work did not cause arcing from cathode to anode for the bond runs used to generate the 800 volt data plotted in figure 5-6. Nitrogen at pressures in the range of 253 Torr to 658 Torr of vacuum was tried to see if the enhancement of heat transfer from the cathode to the glass and other components would have any significant effect either in reducing the required time to reach equilibrium or on the (T, V, t) surface. It was not clear if the nitrogen samples reached equilibrium faster since sample-to-sample variations were so great. However, the maximum voltage applicable before arcing was reduced to less than 400 volts. Within the variations due to the glass and wafer samples, no effect on the T, V, t points were apparent. With other methods which affect the rate of heat transfer to the glass such as discussed in sections 6.2 and 6.3, the only advantage of accelerated heat transfer using nitrogen is to accelerate cooling of the samples after bonding.

An important consideration regarding the ambient during bonding is in maximizing the voltage at which arcing around the edge of the glass occurs. For pressures much above hard vacuum, the breakdown voltage, V_B , of a gas depends on the product of pressure p, and gap size, i.e., d, $p \cdot d$ (Paschen's Law, ref. 6).

Plots of V_B versus $p \cdot d$ for air, N_2 and various other gases are shown in figure 5-8 (ref. 7). These dependences can be qualitatively understood by considering that arcing is caused by avalanching of the gas. As the gap is reduced, the electric field is increased for a given voltage so that electrons attain a higher velocity in a given path length and thus a higher probability of producing ionization upon collision. As the pressure is reduced, the collision probability goes down so that the electrons have a better chance of attaining an energy between collisions sufficient to cause ionization. However, as the pressure and electrode spacing are reduced below some optimum value, the

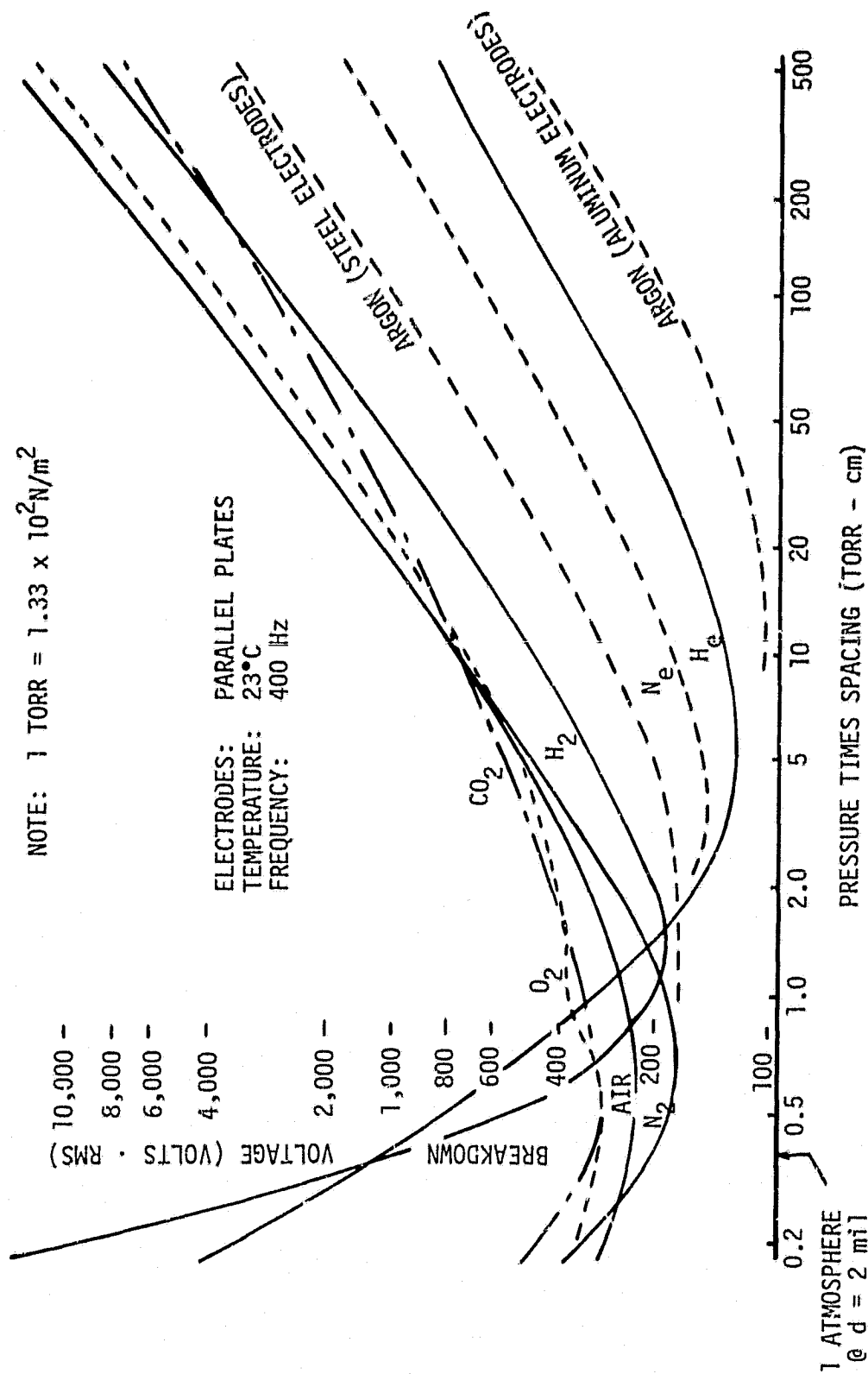


Figure 5-8. Voltage Breakdown of Pure Gases as a Function of Pressure Times Spacing (ref. 7)

probability of any collision at all is reduced to such a level that the required voltage increases with decreasing p.d. At hard vacuum levels, V_B becomes independent of pressure and is more a function of spacing and electrode properties.

The maximum in V_B does not always occur at hard vacuum. For example, figure 5-9, (ref. 8) shows that maximums were found at around 0.1 to 100 μm (Hg) in N_2 . This effect does not appear to be well understood, but it appears that it is dependent on gap length.

Based on dependencies such as described above, it might be expected that manipulations in ambient gas type and pressure could be used to increase the allowable bonding voltage. As discussed in section 6.3 this might have significant advantages for bonding glass to solar cells using the cathode-pillow method.

5.4 GLASS AND SILICON SURFACE TREATMENTS

It might be anticipated that improvements in the bonding process, i.e., lowering of required temperatures, times, etc., to obtain satisfactory bonds, might be made by altering the glass molecular structure or altering the structure of the glass surface to be bonded and the surface to which it must bond. The highly ordered structure of silicon and the well-developed understanding of the physics and chemistry of these structures would seem to lend itself to a somewhat straightforward approach to a study of the phenomena related to bonding to its surface. Glass, however, is a less well understood and more complicated material. Although it is less ordered than silicon, there is a short range order to the structure and the interface with silicon must encompass a transition between the two structures.

The silicon oxygen bond may be the principle factor in this transition zone. Consider the following factors:

1. The oxygen ion is easily polarized both by an electric field and by a variety of other ions.
2. Silicon oxides deficient in oxygen are well known.

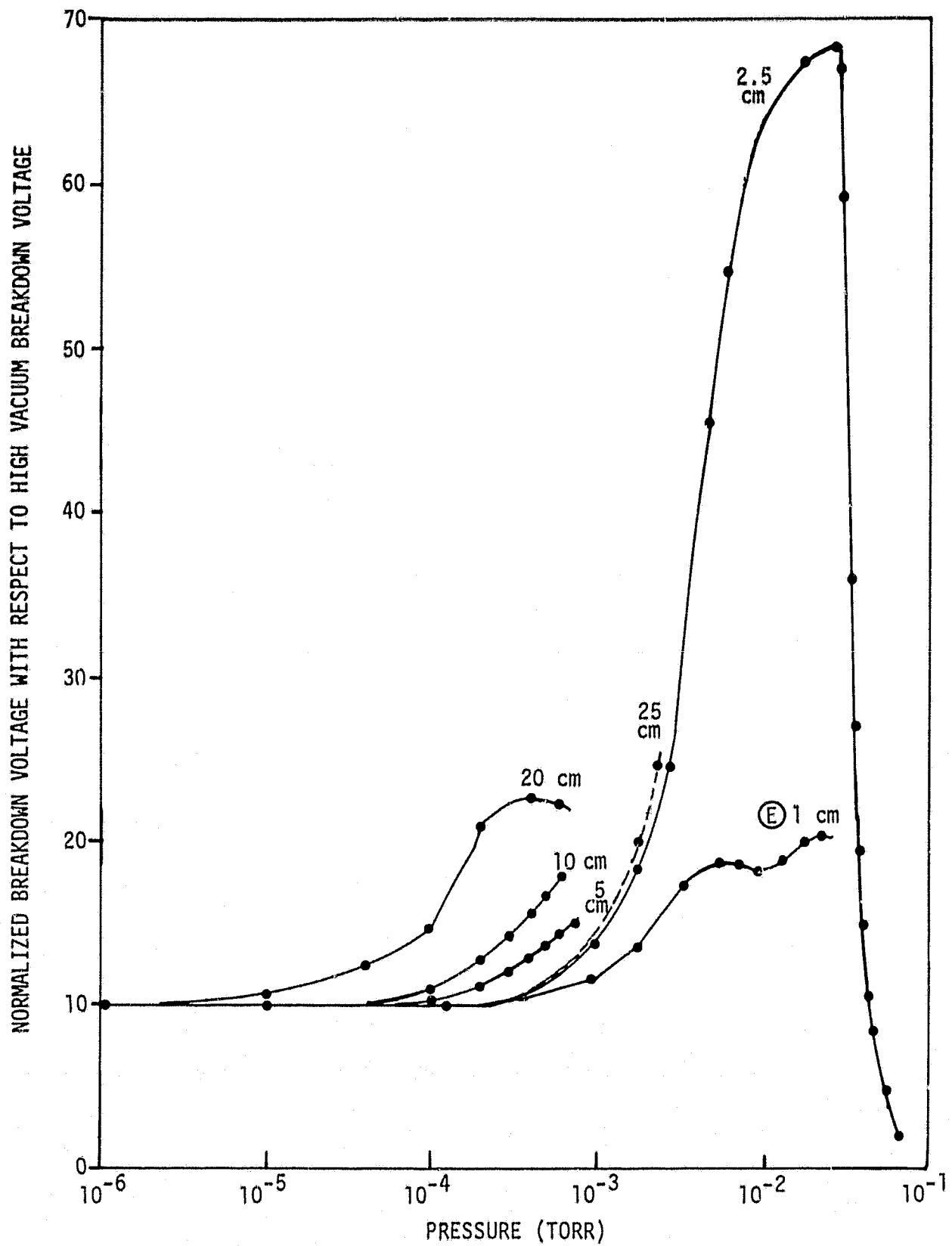


Figure 5-9. Example Low-Pressure Gas Breakdown Voltage Dependence (ref. 8)

3. In the ESB process it is necessary to apply an electric field across the silicon-glass interface such that the silicon is positive. This is the polarity necessary to enhance the production of silicon oxygen bonds.

There are several other known phenomena which are not inconsistent with the speculation in the preceding paragraph. Glass-to-metal seals depend on an oxide surface on the metal or an oxidizer in the glass. It is also necessary that the metal oxide be soluble in the glass or that the metal in the oxide be capable of alloying with or "wetting" the base metal. These phenomena are necessary for enameling metal also. Ceramic tile contains crystalline oxides which gradually change to a glass phase in the glaze producing a strong bond. The fact that glass can be bonded successfully either to bare silicon or to SiO and Ta_2O_5 is, therefore, not surprising.

The function of the electric field may be several fold. First it may polarize the oxygen in the SiO bond and help weaken the Si-Si bonds at the surface of the silicon, causing attraction by forces such as vanderWaal's forces. When silicon ions and polarized oxygen ions approach each other more closely, stronger bonds are formed. Simultaneously, mobile alkali cations will move away from the interface region, making more oxygen available at the bond line, and concentrating alkali oxides toward the outer glass surface. As these regions become polarized, the field spreads laterally, spreading the bond.

It would require an extensive research effort to reach a good understanding of glass-silicon bonding. However, improved technology might be achieved empirically by considering silicon to be the metal in a glass-metal bond and trying those techniques which are known to enhance porcelainizing, glass-to-ceramic, and glass-to-metal seals. A limited and highly empirical investigation was made of a few possibilities as discussed in the following subsections. The results can generally be summarized as "no significant effects observed." There are many other interesting and more sophisticated experiments and treatments that could be tried, however, due to limited time on this program and problems more critical to initial development of a viable ESB bonding approach for solar cells the experiments were limited to those discussed below.

5.4.1 Ta₂O₅ AR-Coating Thickness

Since the AR-coating is a dielectric material, it is reasonable to assume that it might behave electrically in a manner similar to the glass. If the AR-coating has significant ionic conduction with neutralization of the displaced ions similar to the glass as was discussed in section 2.1, the residual negative space charge might screen out some of the attractive electrostatic force between the glass and silicon. Depending on the ionic content of the AR-coating and its thickness it was postulated that it might become the controlling factor in the ESB process. Observations with 2-mil Solarex cells having different colors of SiO_x layers (suggesting that the SiO_x ranged between 950 Å and 1620 Å thick) supported this possibility. ESB bonds were established on the surface of the cell type postulated to have 950 Å SiO_x but none were possible on the other type.

Samples were prepared with varying thicknesses of Ta₂O₅ coatings to establish the role of the coating thickness in the ESB process. The samples were prepared by NASA Lewis Research Center with a number of thicknesses covering the range of 385 Å to 760 Å (see section 3.2). To eliminate the variable of surface texturization density, these samples were made from polished silicon wafers. Bonding conditions were determined which gave partial bonding on a macroscopic scale on these samples and then two samples of each available thickness were bonded using these conditions. The conditions were:

$$P = 15 \text{ psi}$$

$$V = 600 \text{ V}$$

$$C/H \text{ Temp.} = 475^{\circ}\text{C}$$

$$A/P \text{ Temp.} = 250^{\circ}\text{C at start of bonding}$$

$$\int I(t) dt = 0.5 \text{ mA-min}$$

Assuming that the degree of bonding is proportional to $\int I(t)dt$, if other conditions are constant (see section 5.1.3), glass variations should have been cancelled by using this integral instead of time.

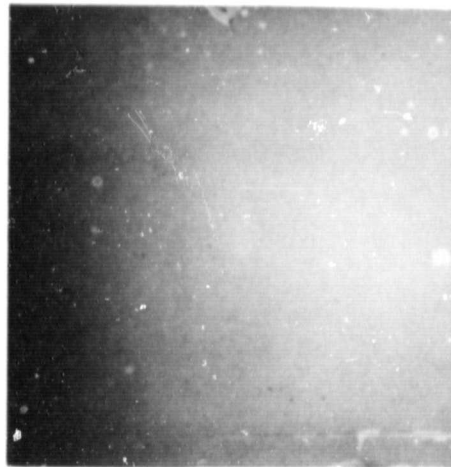
The results showed remarkably identical degrees of macroscopic bonding for all available sample thicknesses. Extreme results are shown in the photographs of figure 5-10. The darkest regions on each sample are bonded and lighter regions are unbonded. Polished silicon wafers without any AR-coating were also bonded under these conditions and showed essentially complete bonding (also shown in figure 5-10). Since the bare wafers were from a different source and of different thickness, it is not certain if the effect is entirely due to the lack of AR-coating; but if it is, the indication might be that the AR-coating affects the chemical bond but not the field buildup.

5.4.2 Ion Exchange

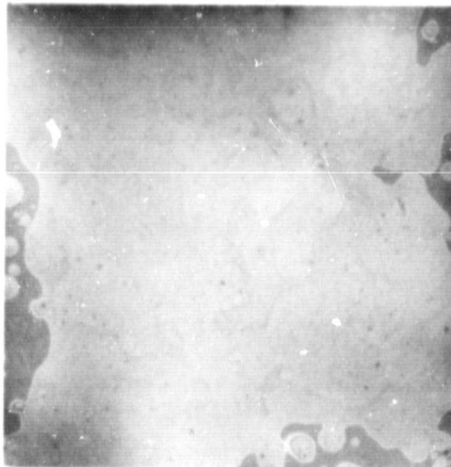
It was speculated that the current during the bonding process might be the result of the movement of relatively mobile Li^+ ions in the 7070 glass. This was in part based on the observation that bonding could not be achieved with an old batch of 7070 glass thought not to contain Li^+ as opposed to newer 7070 which did bond and did contain Li^+ . If the speculation were true, it might be that exchanging mobile Li^+ ions for less mobile Na^+ ions in the glass would result in enhanced bonding. The technique tried for increasing the Li^+ ion content is commonly known as ion exchange. If an insoluble solid is brought in contact with a molten solution, its surface can exchange ions. The ion exchange process is used routinely in the glass industry in chemical tempering of glasses (ref. 9). The tempering is accomplished by exchanging potassium ions from a molten potassium nitrate solution for the sodium ions in the surface layers of the glass. This exchange of larger potassium ions for smaller sodium ions creates compressive forces in the glass surface and effects the tempering.

On this program, glass samples were treated by immersion in solutions of molten, $\sim 300^\circ\text{C}$, LiNO_3 for varying periods of time. It was found that if immersion was maintained too long (usually ≥ 2 hours), the glass would become etched and milky in appearance. Since this was considered intolerable, the immersion time was reduced to a level just short of causing this effect (usually about 1 hour). To avoid confusion due to the sample-to-sample variation in the glass, samples were immersed only halfway into the molten LiNO_3 . Samples were pretreated by cleaning with detergent and rinsing in distilled H_2O and also by immersion in H_2O_2 . It was assumed, based on visible change in the glass color (reflection) in the treated areas, that the glass composition had been changed by the treatments.

BARE WAFER



385 Å Ta_2O_5



760 Å Ta_2O_5

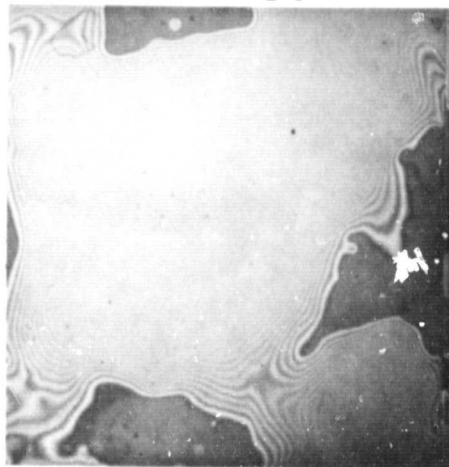


Figure 5-10. Example of Bond Degree Versus Wafer Surface Coating Thickness (Using Identical Bonding Conditions)

Samples treated as described above were bonded to Ta_2O_5 coated etched wafers using conditions which normally lead to marginal microscopic bonding. If the treatment was of any value, the treated portions should have bonded to a greater microscopic degree than the untreated portions of the samples. No significant difference was detectable.

5.4.3 Cation Adsorption

The configuration of tantalum in Ta_2O_5 might strongly affect the adhesion of SiO_2 with Ta_2O_5 antireflection layers. For example, the SiO_2 - Al_2O_3 system is very compatible and bonds readily since both Si and Al are in tetrahedral configurations. On the other hand, it is known that SiO_2 and Cr_2O_5 do not adhere, probably due to the octahedral configuration of Cr which results in poor "mixing" of these systems. Based on such considerations, treatment of the glass surface with metallic ions to form better matching properties was thought to be one possible means of improving the bondability of cover glasses.

It has been observed that glass surfaces exposed to aqueous solutions of heavy metal ions will adsorb varying amounts of the metal ions (ref. 10). In an attempt to introduce metallic ions which might have better matching properties with the Ta_2O_5 layer, glass samples were half immersed in saturated aqueous solutions of metallic salts. The salts tried included $MgCl_2 \cdot 6H_2O$, KCl, $CdCl_2$, Ta_2Cl_5 and $AlCl_3$. Some change in the glass took place for most of these treatments as evidenced by visible changes in the reflective properties of the glass. The treated samples were bonded to Ta_2O_5 -coated etched wafers using conditions leading to partial bonding. In no case was there any significant difference in the degree of bonding in the treated versus untreated sides.

5.4.4 Cleaning With H_2O_2

Cleaning processes are known to be very important in glass-to-metal bonding and wetting. Because of this and also due to the possible significances of interstitial oxygen atoms in the bonding process, some samples were cleaned in an ultrasonic bath of 30 percent H_2O_2 (a strong oxidizing agent) for times ranging from 1 to 240 hours. As with many other treatments, a visible change in glass color and or reflectivity occurred indicating that the treatment had changed the glass. No effect was noted in the degree of bonding between treated and untreated parts of the glass in any case.

5.5 DELIVERABLE SAMPLES/SELECTION OF OPTIMUM BONDING CONDITIONS

Nine samples were prepared and delivered to NASA Lewis Research Center for evaluation using "optimum" bonding conditions. In defining and selecting optimum bonding conditions it was assumed that the requirement of minimizing solar cell damage while achieving an acceptable bond would best be accomplished by minimizing the temperature-time product.

The results presented in the preceding sections show that successful bonding to wafers can be achieved over a wide range of voltages and times for anode temperatures above $\sim 350^{\circ}\text{C}$. It is apparent that the temperature time product can be minimized by applying the maximum voltage. Also due to the small values of $\partial T/\partial t$ at any value of V on the T, V, t surface (see figures 5-6 and 5-7), it would seem that the time-temperature product would be minimized by using a high bonding temperature. The highest allowable cathode temperature was thus used but since nothing was to be gained by letting the anode come to a high temperature before applying the bonding voltage, the voltage was applied at the minimum temperature on the surface. Under these conditions, bonding is proceeding while the anode and thus the solar cell temperature is rising. Due to sample-to-sample variations, a minimum time at any voltage and temperature can not properly be set beforehand. However, the observed correlation between the degree of bonding and bonding current integral suggests that the time can be minimized by specifying the value of $\int I(t)dt$. Based on such considerations, the following procedures were used to prepare samples for delivery:

1. The cathode/heater was brought to 550°C as quickly as possible.
2. A pressure of ~ 15 psi was applied to the anode/pressure foot.
3. A voltage of 600 V was applied when the anode/pressure foot reached 320°C .
4. Bonding was continued until the time integral of current reached 0.5 mA-min.
5. The voltage was removed.
6. The pressure was reduced.
7. The samples were cooled and removed.

Initially the maximum voltage of 800 V was used. In attempting to prepare a number of samples using these conditions, difficulty was experienced

with sporadic arcing between the wafers and the cathode. It was found that a reduction to 600 V alleviated this problem with minimum increase in bonding temperature and time.

An example of the strip chart recordings of temperatures, current, and voltage versus time for these samples was shown in figure 5-4 of section 5.1.3. A summary of the key parameter values for the nine samples is given in table 5-1. All nine samples had about 50 percent bonding on a microscopic basis and 295 percent macroscopically. Five of the samples were subjected to the temperature cycling tests described in appendix A and four were subjected to peel tests described in appendix A. No failures occurred due to these stress tests.

TABLE 5-1. SUMMARY OF BONDING PARAMETERS FOR DELIVERED WAFERS
($\int I(t)dt = 0.5 \text{ mA-min}$)[†]

SAMPLE NUMBER	1	2	3	4	5	6	7	8	9
A/P BLOCK STARTING TEMP (°C)	320								
A/P BLOCK FINAL TEMP (°C)	407	388	357	331	348	341	338	348	348
BONDING TIME (MIN)	7.6	3.9	0.75	0.8	1.3	1.5	0.75	1.3	1.3

[†]See text for other conditions

6.0 TASK II AND III — BONDING GLASS TO SOLAR CELLS

6.1 PRELIMINARY ATTEMPTS AND PROBLEM DEFINITION

The optimum conditions selected in task I and defined in section 5.5 were used in an attempt to bond glass to solar cells. When applied to solar cells, these procedures resulted in no bonding at all. The application of higher pressures, voltages, temperatures and times resulted in some bonding but the results were unsatisfactory. The primary problem in bonding to solar cells of this type was the initial deformation of the glass over the raised contact grids. One solution to this problem would be to develop solar cells with recessed contact grids; however, this increases manufacturing steps and cost. The objective of the present effort was to establish conditions for bonding to existing solar cells, and therefore, means were sought to enhance the deformation of the glass over the grids. Considerable benefit would be gained by raising the temperature of the glass so that it becomes more viscous. As can be seen by figure 6-1, the viscosity of the glass is dropping rapidly with increasing temperature at the temperatures used. Unfortunately, raising the temperature of the glass by simply raising the temperature of the bonder cathode would raise the temperature of the solar cells to a level where damage to electrical properties would likely be intolerable. The ground rules of the present effort, therefore, required that the temperature be kept below 550°C.

Two possible solutions to the above problems, which were within the ground rules of the present effort, were conceived and investigated. These solutions and the degree of success obtained are discussed in detail in the next two sections.

6.2 CATHODE-PILLOW ASSISTED BONDING

Considering the ESB process, with a hard flat cathode, it is apparent that the glass over the contact grid bars must be compressed by the amount of the grid thickness before the glass and semiconductor surfaces can be put into intimate contact as illustrated in figure 6-2a. It was speculated that due to the thinness of the glass relative to the spacing between grid bars, it might be easier to bend the glass between the bars than to compress it over the bars. It was conceived that if a C/H surface were provided with appropriate viscosity or

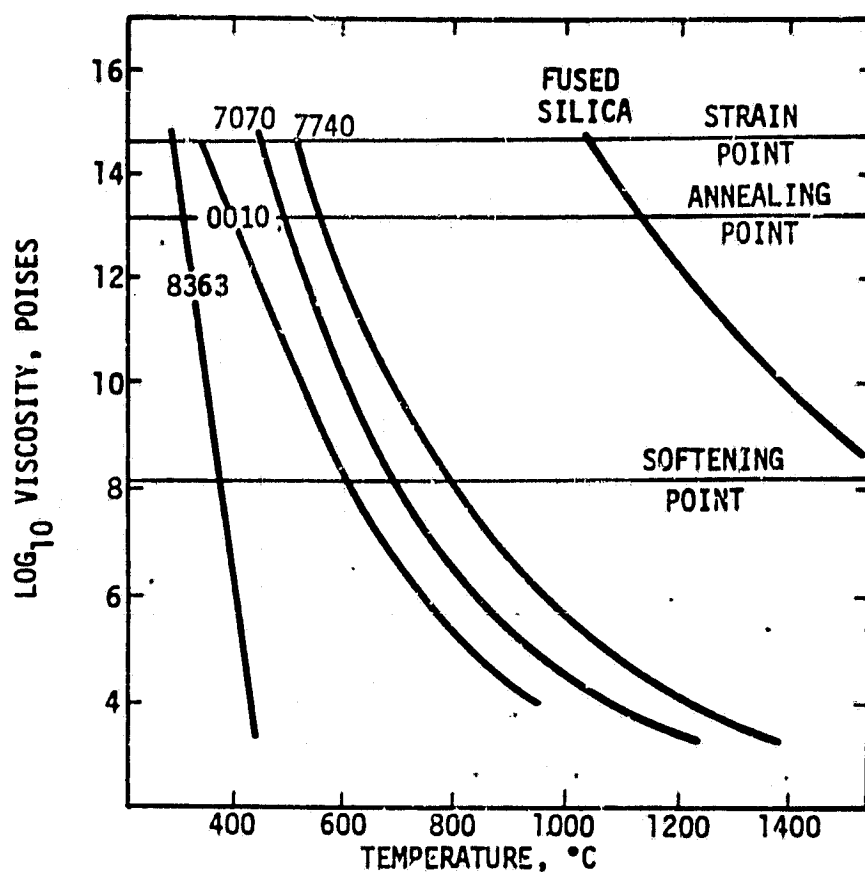


Figure 6-1. Viscosity vs. Temperature for Some Commercial Glasses

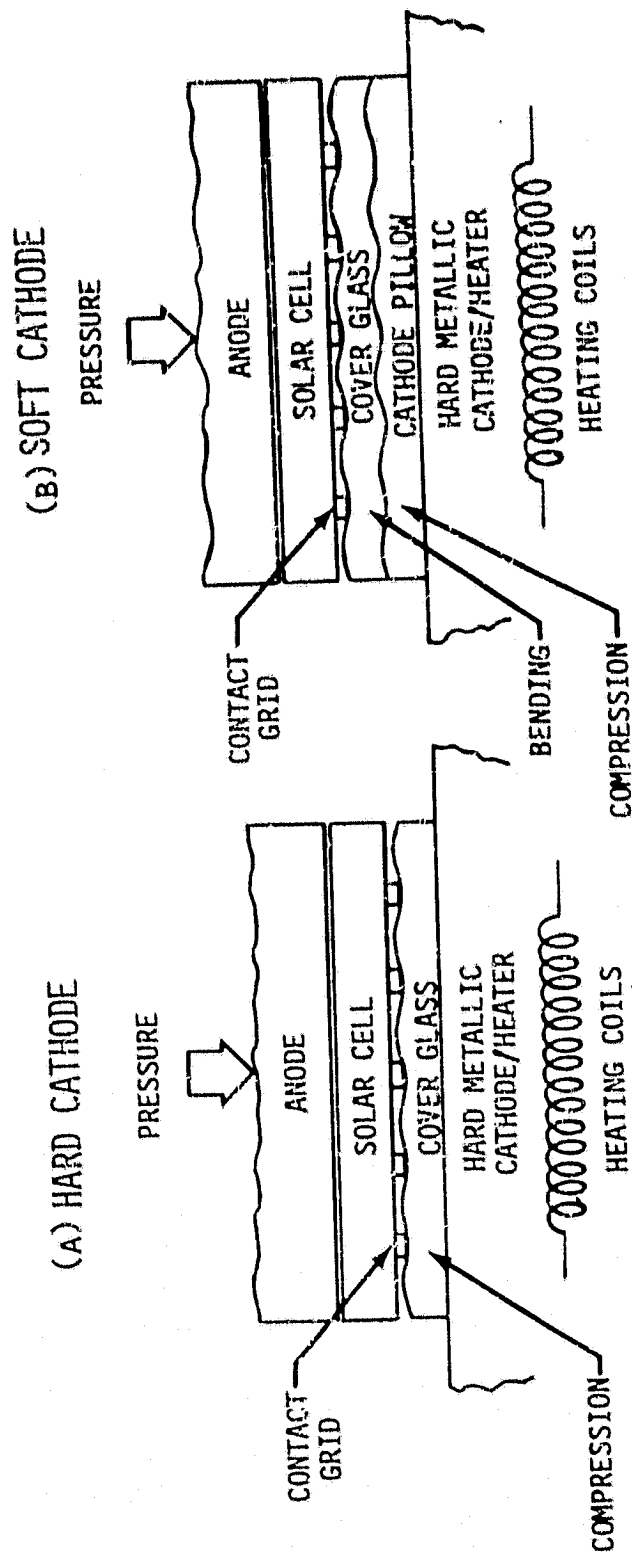


Figure 6-2. Physical Features of ESB Process Using Hard and Soft Cathodes

compressibility, such glass bending might be achieved as illustrated in figure 6.2b. The term, cathode pillow, was applied to this soft cathode concept.

In developing a cathode pillow with the desired properties, forming a pillow of soft material or gas captivated by a thin conducting membrane was considered. It seemed that a more straightforward approach might be to find a conducting material having the appropriate compressibilities or viscous properties so that it could be used without a captivating membrane. Soft copper and aluminum alloys were tried without success. Metals which are softer than those tried have melting points which are below the required bonding temperatures and could not be used. Finally, it was speculated that since graphite (which is an excellent conductor, able to withstand high temperature) comes in so many forms there might be some form with the desired properties. A product of Union Carbide called "Grafoil" was found to have the desired properties. This material comes in two grades, GTA and GTB, and in several thicknesses. Both grades were tried in 0.005" and 0.010" thicknesses. The comparisons were not exhaustive, however, it appears that 0.005" GTB gives the best results.

An initial problem with the method was that arcing around the edges of the glass was more prevalent. Apparently as the sample is pressed into the pillow, the distance between the conducting solar cell and conducting pillow is diminished. To reduce this problem, pillows were cut slightly smaller than the glass size and an alteration to the bonder was fabricated to closely align the pillow, glass, and solar cell. A cross-sectional sketch depicting the essential features of this apparatus is shown in figure 6-3. One drawback to such a method is that it either requires extremely close tolerances or acceptance of a strip of unbonded glass around the periphery of the sample where the pillow does not extend. One possible solution which might be better would be to utilize glass covers which are bigger than the solar cells. The approach seems particularly suitable for bonding cells with contacts on the back side. A number of cells might be bonded at once to a large sheet of glass and either diced out of the glass after bonding or perhaps fabricated directly into a solar array.

Photographs of samples typifying the superiority of results obtained with a cathode pillow and with hard cathodes are shown in figure 6-4. It was determined by bonding of a number of rectangular grid cells using a soft cathode that acceptable bonds are achieved using the conditions: $P \sim 55$ psi, $V \sim 600$

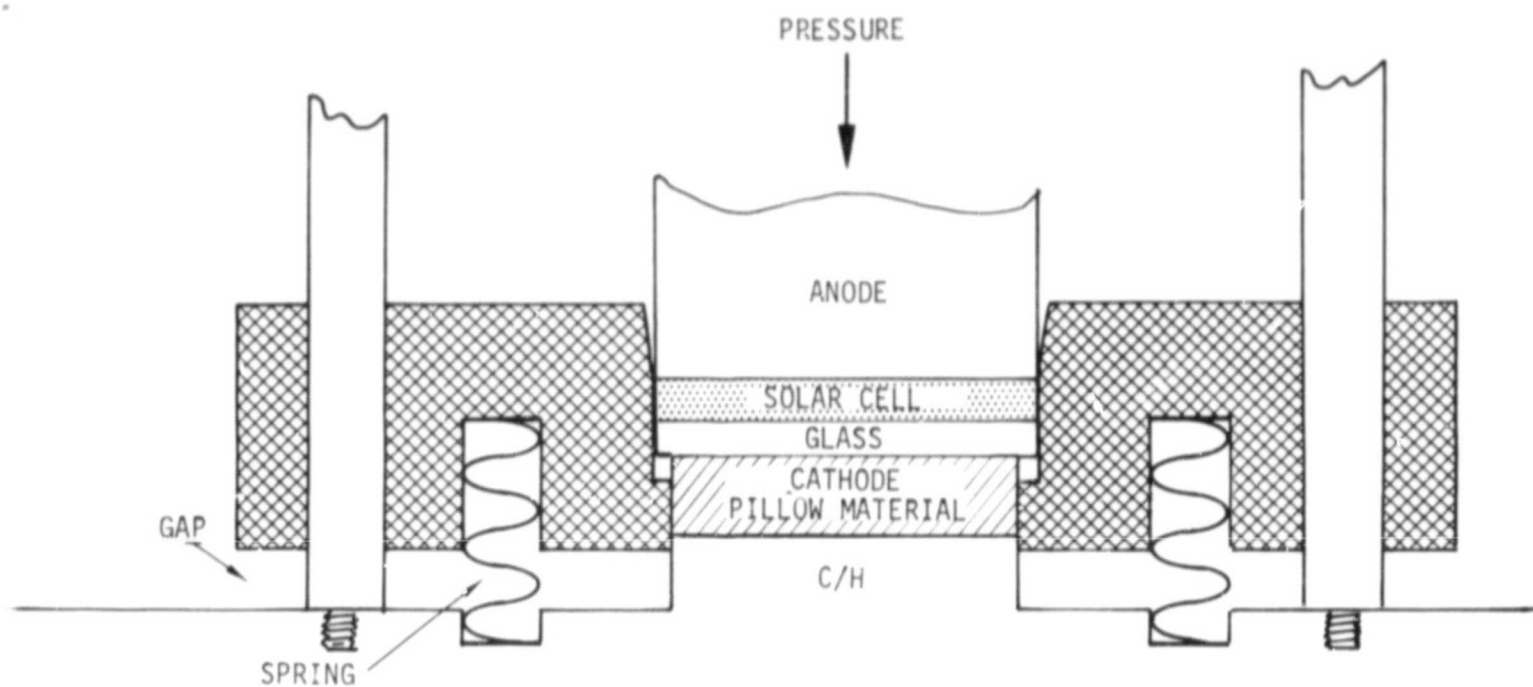
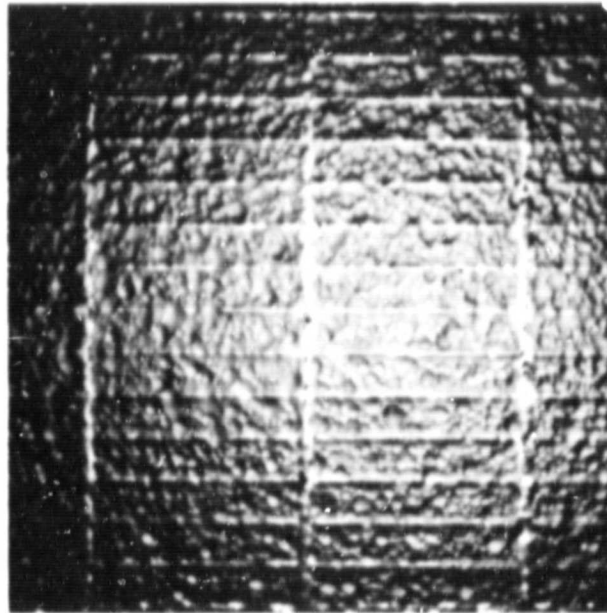


Figure 6-3. Physical Features of Altered Bonder Head Showing Cathode Pillow and Alignment Mechanism

(a) CATHODE PILLOW



(b) HARD CATHODE



ORIGINAL PAGE IS
OF POOR QUALITY

Figure 6-4. Example Solar Cells With Glass Bonded Using Hard and Soft Cathode

volts, $\int I(t)dt \sim 3$ mA-min, and starting the bonds at anode temperatures of 415°C with C/H temperatures of about 550°C. Anode temperatures usually level out at about 495°C before the bonding voltage is removed. Bonding times under these conditions are typically less than 3.0 minutes. The degree of microscopic bonding was found to increase considerably with further increases in $\int I(t)dt$, however, the cell degradation also increases significantly. It has not yet been determined if the benefits of this increased degree of microscopic bonding are worth the extra penalty in electrical degradation of the cells.

An initial ground rule for this program was that the anode pressure be kept below ~ 50 psi. Most of the solar cell bond runs were made at an estimated 55 psi but a number of cells were bonded using about 75 psi since no deleterious mechanical effects of this higher pressure resulted when using cathode pillows and since for cells with raised contact grids, higher pressures should result in greater initial contact and more complete bonding. It is not clear from the results whether or not 75 psi was significantly better than 55 psi.

Good bonds were achieved on most of the cells bonded using the conditions discussed in the last two paragraphs. Some difficulty was experienced with shorting during the bonding process and it appears that more work needs to be done to solve this problem. When the samples short during a bond run, the electrical parameters are unduly degraded. It is believed that this is the result of severe localized heating from the electrical arcs at points of break down around the edges of the cover glass. For samples which did not arc during bonding, electrical parameter degradation is primarily manifest in a reduction of I_{sc} and a consequent reduction in P_{max} as illustrated in figure 6-5. One cell was measured with an unbonded cover glass held in front. That cell showed a reduction of about 5 percent in I_{sc} and 6 percent in P_{max} due to a reduction in transmitted light. The minimum degradations noted so far for samples bonded by the ESB process using the conditions discussed in the last two paragraphs above were about 9 percent in I_{sc} and 13 percent in P_{max} . Thus, some thermal degradation has apparently occurred. Parameter degradations are summarized in table 6-1 for ten samples bonded under the conditions discussed in the last two paragraphs. The mean degradations were: $I_{sc} = 13\%$, $V_{oc} = 2\%$, $P_{max} = 20\%$, and $FF = 7\%$.

The above results pertain to the rectangular grid samples only. Herringbone samples were more difficult to bond and the bar grid samples did not

EXAMPLE IV PLOTS

S/N : 30	LEVEL : 0	1
TEMP: 25 C	ISC(MA) : 147.6	135.9
AREA: 4 CM^2	VOC(MV) : 601.9	598.2
INT. : AM0	PMAX(MW) : 69.6	63.5
	F.F. : 0.764	0.767

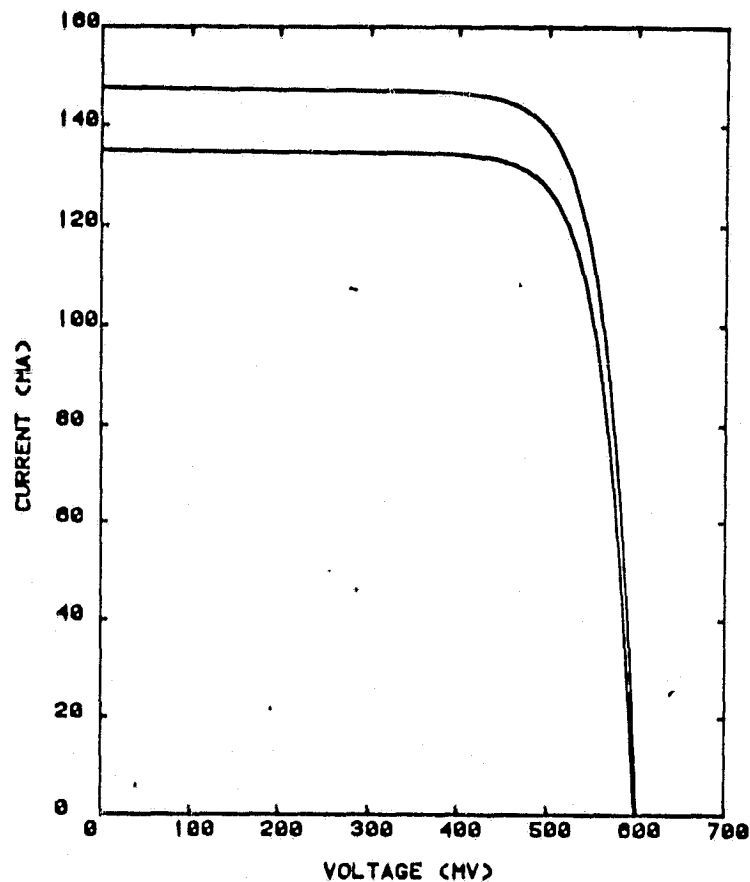


Figure 6-5. Example of Best Case Electrical Parameter Degradation Caused by ESB

TABLE 6-1: TABULATION OF PRE- AND POST-BOND ELECTRICAL PARAMETER VALUES
FOR SAMPLES WITH $\int I(t)dt = 3 \text{ mA-min}$

(Note: Samples showing electrical breakdown during bonding excluded.)

SAMPLE I.D.	BOND TIME	PARAMETER NAME	PRE-BOND	POST-BOND	CHANGE PERCENT
104	2.0	I _{sc}	150.0	136.4	9
		V _{oc}	601.5	594.9	1
		P _{max}	69.8	60.8	13
		FF	0.774	0.749	3
122	2.3	I _{sc}	145.6	125.2	14
		V _{oc}	600.3	590.8	2
		P _{max}	68.2	55.3	19
		FF	0.780	0.748	4
121	2.2	I _{sc}	146.5	130.2	11
		V _{oc}	601.4	591.0	2
		P _{max}	68.3	54.3	20
		FF	0.775	0.706	9
119	2.0	I _{sc}	147.2	129.1	12
		V _{oc}	601.7	592.7	1
		P _{max}	69.6	54.7	21
		FF	0.785	0.714	9
115	2.0	I _{sc}	147.3	126.1	14
		V _{oc}	602.3	587.3	2
		P _{max}	70.6	51.3	27
		FF	0.795	0.693	13
114	2.2	I _{sc}	144.7	122.8	15
		V _{oc}	604.5	578.6	4
		P _{max}	68.9	51.2	26
		FF	0.788	0.720	9
110	2.2	I _{sc}	147.7	125.6	15
		V _{oc}	605.5	596.9	1
		P _{max}	71.3	58.7	18
		FF	0.797	0.783	2
108	2.0	I _{sc}	147.9	124.3	16
		V _{oc}	601.0	590.9	2
		P _{max}	67.8	52.2	23
		FF	0.763	0.710	7
107	2.0	I _{sc}	149.1	134.7	10
		V _{oc}	602.6	591.7	2
		P _{max}	70.0	58.0	17
		FF	0.779	0.728	7
105	2.8	I _{sc}	150.0	133.5	11
		V _{oc}	605.3	597.3	1
		P _{max}	71.5	58.8	18
		FF	0.781	0.737	6

bond at all under conditions which led to good bonds on the rectangular grid samples. The reasons for these differences have not yet been fully investigated, but seem to be due to thicker, more closely spaced grid bars for the herringbone and a radically more complex semiconductor surface structure for the bar cells. (See section 3.3 for a description of the geometrical aspects of the three cell types.)

As shown by the above data, some cell degradation due to the thermal soak during the ESB process occurs even under the shortest bonding times. While this degradation was slight for some of the cells, it was significant for others. With the cells and glass that were used, it is evident from the observed degradations that if the variations in the glass and cells could be controlled so that the best conditions were always present degradation could be kept to less than about 9%, 1%, 9% and 1% in I_{sc} , V_{oc} , P_{max} and FF, respectively. Considering the actual time-temperature conditions used to obtain good bonds, there should be other cell designs which could be easily bonded with insignificant damage.

Damage might also be reduced significantly by optimizing the speed of heat up of the glass prior to bonding while keeping the cell cool and optimizing the cool down after bonding. Such manipulations would require bonder redesign. This was beyond the scope of the present effort. A preliminary investigation of another approach was made and is discussed in the next section.

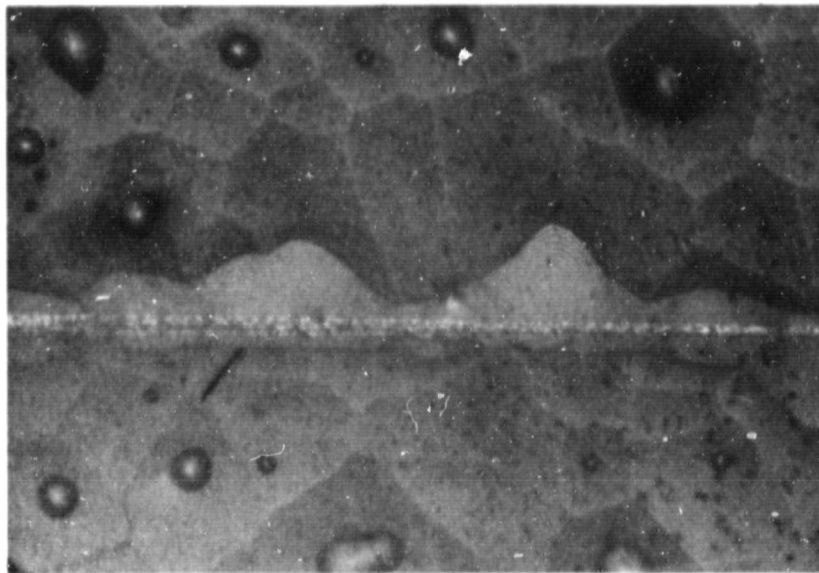
6.3 ELECTRO-OPTICALLY ASSISTED ESB

In an attempt to develop means of further reducing the thermal stress to the cells, a technique using a pulsed laser beam to heat the glass to the softening point in a very short burst was conceived. The technique would involve a background temperature sufficient to allow ion migration in the glass to establish an electric field between the glass and cell in a manner similar to the standard ESB technique. The background temperature would be maintained below the level at which the solar cell would degrade. The laser pulse would then soften the glass allowing the electric field to form the glass into the solar cell surface and around the contact grid. During subsequent cool down the interface would be bonded by the standard ESB process. It was calculated that this could be accomplished with the cell temperature above the threshold temperature for degradation for times on the order of seconds rather than minutes.

Exploratory tests were performed to establish the feasibility of this technique. The cell-glass combination was mounted in a "picture frame" which clamped it together around the edges and permitted the application of bias voltage across the cell and glass as required for the ESB technique; however, electrical contact was only made around the extreme perimeter of the assembly by the "picture frame" clamp. The clamp was then mounted in a thermally insulating holder inside a vacuum chamber and bias voltage was applied. Background heating to 350°C was provided using an incandescent light beam concentrated onto the back of the solar cell. This shuttered light beam required about five seconds to heat the cell-glass assembly from room temperature to 350°C as indicated by a ribbon thermocouple between the cell and the glass. A CW CO₂ (10.6 μ m) laser beam was then directed onto the glass surface through a shuttering mechanism which allowed continuous variations of the exposure time from $\sqrt{3}$ ms to 30 seconds. Several exposures were made and it was found that with the laser intensity available ($\sqrt{20}$ watts/cm²) a pulse of about one second duration would soften the glass. As observed through a window in the vacuum chamber, in the configuration described, the glass would first buckle upward away from the cell surface during heating. When the softening point was reached the glass could be observed to instantaneously collapse into the cell surface as would be expected if an electric field were present. At this point the current across the assembly, monitored by a chart recorder, increased dramatically (on the order of mA) and after a short interval the assembly would short apparently signaling breakdown of the glass. Examination of the cell and cover glass indicated that the glass had deformed around the contact grid bars and that bonding had occurred around the periphery of the cell to a distance of about 1/8 inch inside the periphery of the "picture frame" clamp where the voltage was applied. Evidence of electrical breakdown was observed near the edge of the glass under the electrode-clamp assembly.

A photomicrograph of the resulting bond is shown in figure 6-6a as compared to that of an ESB bond produced using the "cathode" pillow technique shown in figure 6-6b. It appears that the bonding produced by the pulsed laser technique is more complete on a microscopic scale and the deformation around the contact is more complete than that obtained without laser heating. This bonding was accomplished in a very short time interval (< 1 s following the laser pulse).

(a) LASER HEATING



(b) CATHODE PILLOW

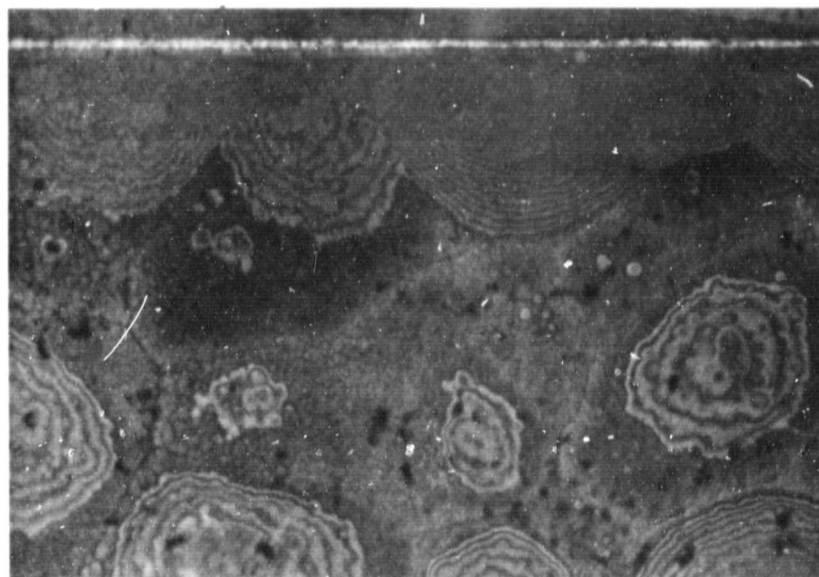


Figure 6-6. Comparison of Microscopic Bonding Using Cathode Pillow and Laser Heating

So far, such laser bonding has not been achieved over a large cell area. This is no doubt due to lack of uniformity in the laser beam. The desired uniformity should be obtainable with further effort. Although further work is needed to fully develop the parameters and optimize the configuration, it appears that laser pulse softening of the glass can enhance the ESB technique. The advantages offered include better conformation between the glass and the silicon surface and greatly reduced bonding times which should minimize or eliminate thermal degradation of electrical parameters.

6.4 DELIVERABLE SAMPLES

Deliverable samples were prepared using the cathode-pillow method. Of the three cell types available, only the rectangular grid type yielded good bonds on a fairly consistent basis. There were 109 rectangular grid cells supplied by NASA-Lewis Research Center. Several cells were expended in process development and some were broken by handling. At the end of the program, 76 of the bonded cells were judged acceptable on the basis of a naked eye physical examination of mechanical bond integrity. Out of these 76 samples about 15 were judged to be of slightly inferior quality compared to the others. Four of the best samples and one of the samples having a slightly inferior quality were put through the screening tests described in appendix A. Of these, no samples failed. Also, 15 samples were used directly for radiation effects testing on contract NAS3-22222. The remaining cells were sent directly to NASA-Lewis Research Center without further testing.

It was determined that bonds with ≥ 95 percent interface area coverage on a macroscopic scale and ≥ 50 percent coverage on a microscopic scale were adequate to withstand Scotch type 810 tape peel tests and -175°C to $+60^{\circ}\text{C}$ temperature cycling. With this definition of a good bond, the conditions of pressure voltage, temperature and time required to make good electrostatic bonds between ~ 2.8 mil Corning 7070 glass and Ta_2O_5 -coated etched silicon surfaces typical of solar cells were established.

To minimize-thermally induced degradation of solar cells, a minimum bonding time and temperature are required. This is best achieved by using a maximum bonding voltage. For anode pressures of 15 psi and hard smooth cathode and anode surfaces, it was often possible to apply 800 volts at ambient vacuums in the range of $1\text{ }\mu\text{m}$ to $20\text{ }\mu\text{m}$ of Hg without arcing. However, to reliably avoid arcing, a 600 volt bias was found to be more appropriate. For bonding unmetallized wafers, at this voltage, an anode starting temperature of 320°C was adequate with a cathode temperature of 550°C .

A correlation between the total integral of bonding current and the degree of bonding was established. It appears that the current integral is a good parameter to use in determining when bonding voltage should be removed to minimize the bonding time. A value of 0.5 mA-min was found to be adequate for the unmetallized Ta_2O_5 -coated Si surfaces.

In bonding glass to solar cells, deformation of the glass over the contact grid metallization was found to be the dominant problem. This problem was greatly alleviated by employing a "cathode pillow" with the appropriate compressibility. Using such a pillow, the thin glass is bent around the grid as opposed to compressing it over the grid as required with a hard cathode. Maximizing the anode pressure with this method yields significant benefits. Anode pressures of ~ 55 psi were adequate but anode pressure up to ~ 75 psi seemed to produce slightly better results with no deleterious effects such as breakage. Enhanced arcing around the edges of the glass as the glass was pushed into the pillow was a sporadic problem but careful control of cathode pillow size and alignment of all elements were usually successful in allowing arc-free bonding.

Thus far, many good bonds of ~ 2.8 mil glass to 2 mil solar cells have been made with acceptably small thermal degradation of the cells. The best

conditions appear to be ~ 55 to 75 psi, 600 volts, a C/H temperature of 550°C , an anode starting temperature of 415°C and a total bonding current integral of ~ 3 mA-min. Bond times for these conditions were typically 1 to 3 minutes.

Additional softening of the glass during the bonding process using a short burst of laser heating was achieved over a small region of a solar cell. This procedure shows promise for improving the bond quality while reducing the cell-thermal stress. The area heated showed more complete bonding than bonds made without laser heating; and further, the bond was achieved in about one second as opposed to minutes. Although further development is required to determine if the laser method is practical and to optimize the process, it is possible that the ESB procedure could be refined to the point where no thermal damage to solar cell electrical properties would result even for the most sensitive cells.

Investigations of the effects of Ta_2O_5 AR-coating thickness and various glass treatments indicated no significant effects on bonding except for enhanced bonding in polished silicon samples with no Ta_2O_5 coating. Inherent variations in the glass, however, were quite significant. These were manifest as variations in the rate of heat transfer and the bonding current under fixed bonding conditions. As a result, to obtain the same degree of bonding from sample to sample, different bond times were required resulting in different degrees of cell degradation. Variations in required bond time of an order of magnitude were observed with other conditions constant. It is thought that the observed variations are due to differences in glass composition, glass thickness, and glass surface irregularities but these factors have not been experimentally investigated.

In short, it appears from the results of this study that the electrostatic bonding process presents a viable technique for bonding thin glass to solar cells. It appears that good bonds can be made to at least one type ("rectangular grid," see section 3.2) of existing thin etched surface Ta_2O_5 coated solar cell with as little as 9% degradation in I_{sc} and 13% degradation in P_{max} using the cathode-pillow method. With further optimization in heat-up and cool-down procedures, this damage should be even further reducible. Other solar cells tried, for example those having extremely jagged texturized surfaces, would not bond at all under the same conditions that led to good bonds on etched surfaces. On the other hand, cells with recessed grids or polished Ta_2O_5 coated silicon surfaces would bond under much less severe temperature and time conditions.

Additionally, bonding using laser heating to assist in the initial glass deformation should be achievable on fairly irregular surface cells with no thermal effect on electrical properties.

The ESB processes should be particularly useful in producing solar arrays when a number of cells can be bonded at once to a large glass sheet if cells with back-side contacts are available. The process should be particularly valuable for systems using thin glass and cells to maximize the power-to-weight ratio since the weight of the adhesive layer is eliminated and also since handling can be minimized. It is recommended that further studies be performed to establish if the laser assisted ESB process is practical and further optimize the cathode pillow method. The reasons for the sample-to-sample variations should also be investigated so that means for producing glass having optimum qualities can be identified.

8.0 REFERENCES

- 1) Kirkpatrick, A. R., Kreisman, W. S., and Minnvcci, J. A., Stress Free Applications of Glass Covers for Radiation Hardened Solar cells and Arrays, AFAPL-TR-77-28, May 1977.
- 2) Wallis, G., and Pomerantz, D. I., "Field Assisted Glass-Metal Sealing," Journal of Applied Physics, Vol. 40, No. 10, p.p. 3946-3949, Sept. 1969.
- 3) Younger, P. R., et al., Integral Glass Encapsulation for Solar Arrays, Interim Report No. 1, JPL Contract No. 9544521, Nov. 1977.
- 4) Wallis, G., "Field Assisted Glass Sealing," Electrocomponent Science and Technology, Vol. 2, No. 1, pp. 45-53, 1975.
- 5) Hutchins, J. R., and Harrington, R. V., Glass, Corning Glass Works, Reprinted from Encyclopedia Of Chemical Technology, 2nd Edition, Vol. 10, p. 542, 1966.
- 6) Alston, L. L., High Voltage Technology, Oxford University Press, 1968.
- 7) High Voltage Design Guide For Airborne Equipment, Boeing Aerospace Co., AFAPL-TR-76-41, June 1976.
- 8) Cooke, C. M., "Residual Pressure and Its Effects On Vacuum Insulation," Proceedings Second International Symposium On Insulation Of High Voltages In Vacuum, p. 181, 7-8 Sept. 1966.
- 9) Hutchins III, J. R., and Harrington, R. V., Encyclopedia of Chemical Technology, Vol. 10, 2nd Edition, Kirk-Othmer, Ed. (Wiley and Sons, New York, 1966).
- 10) Weyl, W. A., and Marboe, E. C., The Constitution of Glass, Vol. II (John Wiley and Son, New York 1967).

APPENDIX A: MECHANICAL SCREENING TESTS

A.1 TEMPERATURE CYCLING

A requirement of this program was that a number of samples be subjected to 10 cycles of temperature between the extremes of $+60^{\circ}\text{C}$ and -175°C with $dT/dt = 25^{\circ}\text{C}/\text{min}$ in the excursions and five-minute soaks at the extremes. Since no apparatus was available for this task, equipment had to be developed for this effort. The mechanical aspects of the apparatus are depicted in figure A-1. The samples were mounted in slots in a wooden rack. A cover glass bonded to a silicon wafer having a 1-mil ribbon thermocouple bonded between the glass and the silicon were mounted in the rack.

The samples were alternately raised into a heating chamber and lowered to the surface of a liquid-nitrogen reservoir. This vertical motion was accomplished via a cord, pulley, and motor. The controller represented in figure A-2 was designed and fabricated to control the motor. The circuitry sensed the thermocouple signal, compared it to a built-in time dependent waveform, and raised or lowered the samples according to the desired temperature-time profile. An example control waveform and cell temperature waveform are shown in figure A-3.

A.2 PEEL TEST

Another requirement of this program was that samples be subjected to a peel test to ensure that the covers do not yield to sudden complete parting at the interface. Peel tests are typically specified for solar cells using Scotch-brand type 810 magic transparent tape. Thus a method based on the use of such tape was developed. A typical peel test method used for thicker cells is to run the samples between two rollers covered by tape which remains for a time on the roller surface while the cell continues out on the tangent which is in common with the two rollers. For the thin fragile 2-mil samples, such a method would not work. Therefore, a means of temporarily bonding the back side of the cells to a flat substrate was devised so that the tape could be stuck to the glass surface and pulled away without breaking the cell. Since it was desired that the cells be recoverable after screening, the bond between the cell and

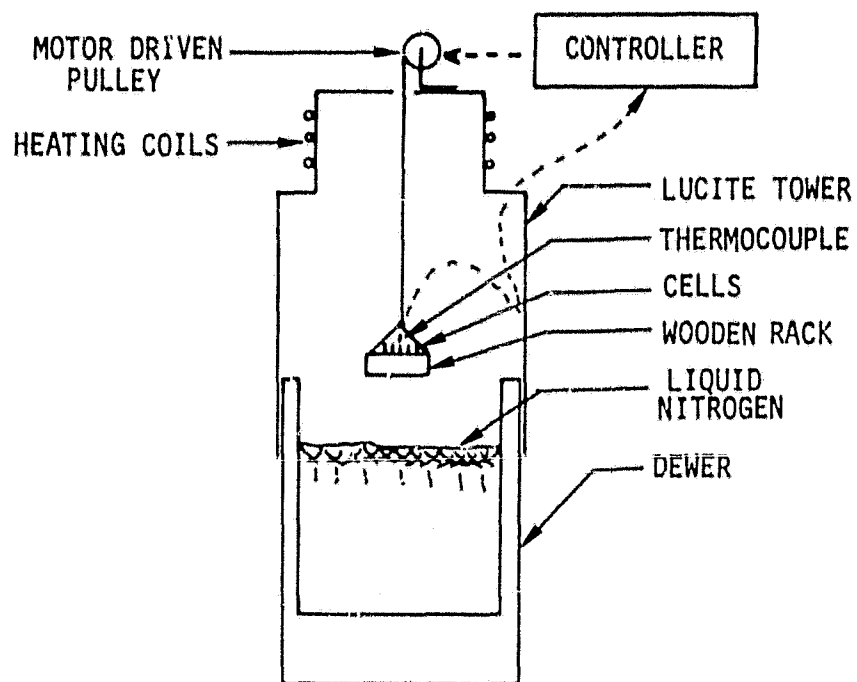


Figure A-1. Temperature Cycling Hardware

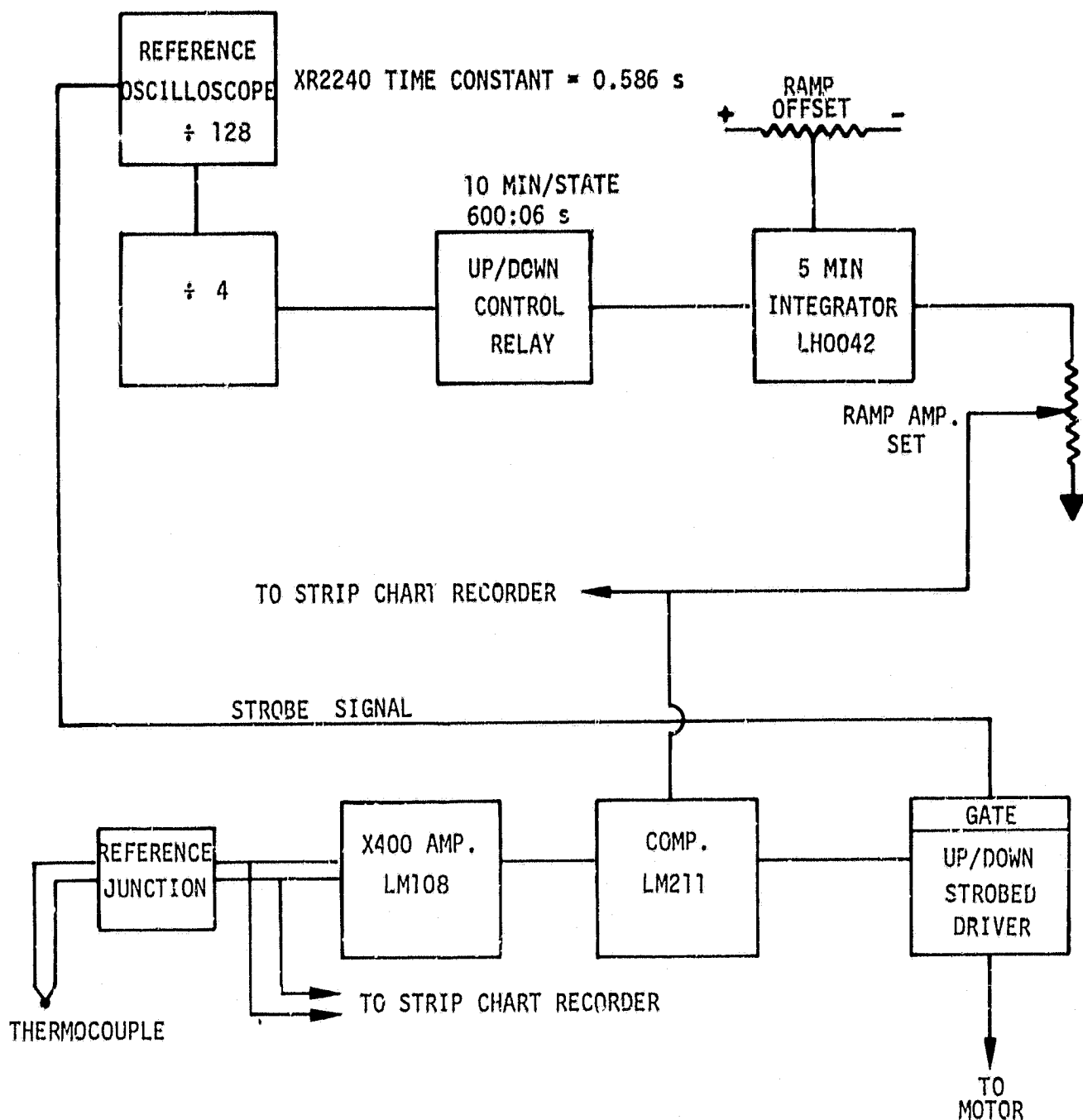


Figure A-2. Functional Diagram of Temperature Cycle Controller

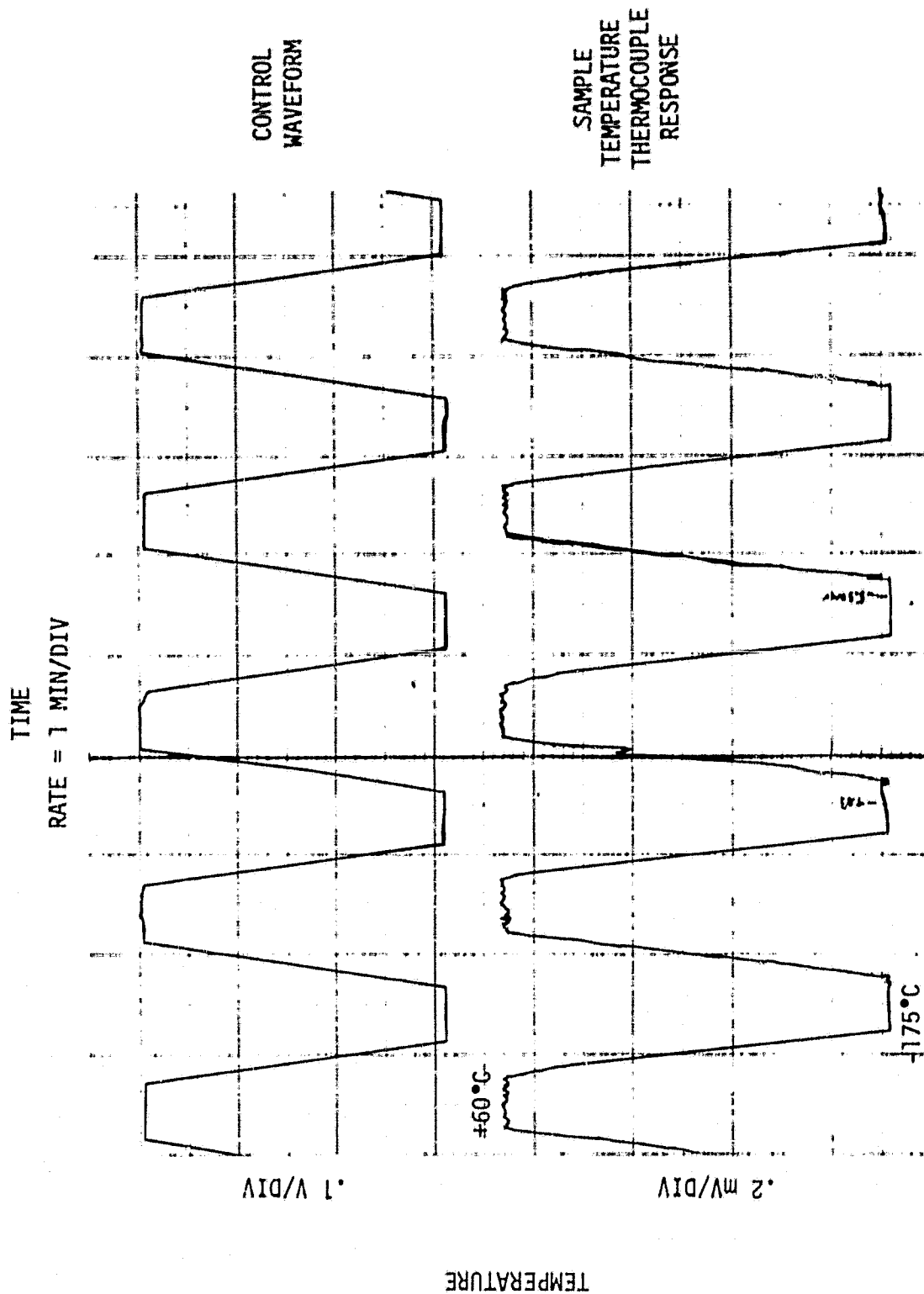


Figure A-3. Example Temperature Cycle Excursions

substrate had to be destructible without destroying the cell. The criteria for a suitable bonding agent then seemed to be that 1) it could easily be removed by some solvent which does not attack the solar cell or glass, and 2) it would release its bond at some temperature below the thermal damage point for the solar cells yet provide a bond at room temperature which was much stronger than the glass-tape bond. Out of several materials tried, black Apiezon wax soluble in trichlorethylene provided the only bond strong enough while having the other required properties. Samples were bonded to a machined flat aluminum block for peel testing using this wax.

An apparatus having the features depicted in figure A-4 was fabricated to facilitate the peel tests. The peel rate was controlled by using a 334 gram weight. This weight was selected as the minimum required to slowly peel the Scotch-brand type 810 tape off a cover glass surface which has been precleaned with trichlorethylene and alcohol. A pull angle of 90 degrees was used.

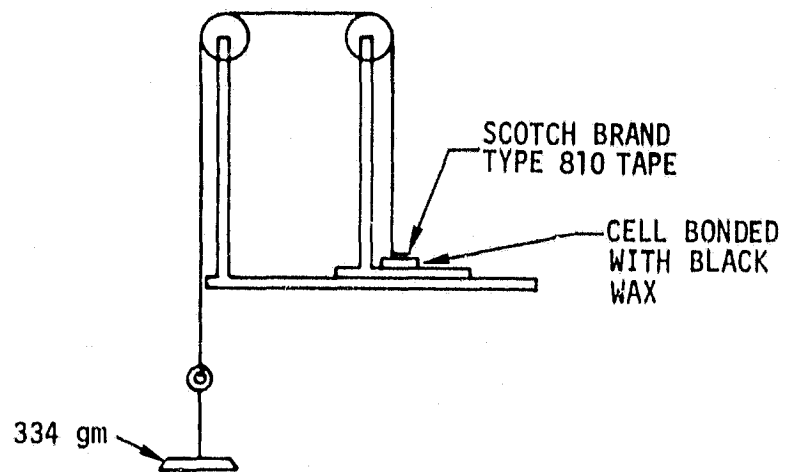


Figure A-4. Peel Test Hardware

APPENDIX B: ELECTRICAL PARAMETER MEASUREMENTS

Solar cell I-V measurements were performed with a computer-controlled test system. A block diagram of the system is shown in figure B-1. Transera A/D and D/A converters have been added to a Tektronix 4051 minicomputer, which acts as the controller to establish cell operating conditions and to record cell output. Under the control of software developed at Boeing, the I-V characteristics of the cells were rapidly scanned with a programmable load bank and the results displayed on a graphic screen for operator inspection. The data was then stored on magnetic tape.

The cells were mounted on a copper block which was maintained at 25°C for all measurements. An X-25 solar simulator and AMO conditions were used. A reference cell provided by NASA Lewis Research Center was placed on the block to monitor the solar-simulator output. The source was then adjusted accordingly. The reference cell short circuit current measured at NASA-Lewis Research Center was 139.7 mA. Our simulator was adjusted each time to give $139.7 \text{ mA} \pm 0.5 \text{ mA}$. The system was programmed to calculate the short circuit current, I_{sc} , the open circuit voltage, V_{oc} , the maximum power, P_{max} , and fill factor, FF.

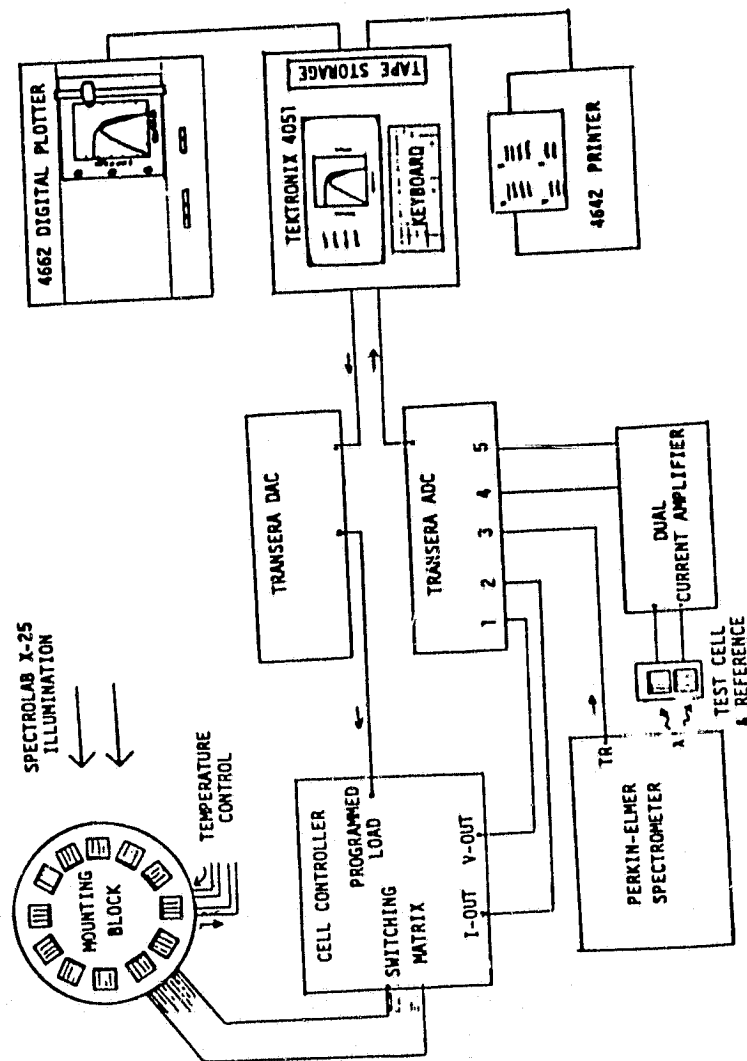


Figure B-1. Solar Cell Parameter Measurement System

APPENDIX C: METHODS FOR FORMATION OF NOTCHES IN COVER GLASSES

It was required that notches be put in the cover glasses to expose the electrical contacts of the finished solar cell structures. Before the final method described in section 4.2 was developed, a number of other methods were tried as discussed below.

Sandblasting

An attempt was made to cut the required notches in the cover glasses by sandblasting. A number of masks for sandblasting were made from Al and Ti foil. Foil was used since the thin glass would break if it was clamped between thick metal surfaces. Although this method showed some promise, the sandblaster available did not have a small enough nozzle so that the masks were cut faster than the glass. Penetration between the mask and the glass was also a significant problem.

Wax Mask and Etch

The conventional method of etching glass is to dip the glass in molten wax, scratch the desired pattern through the wax, and expose the glass to HF fumes or dip it in an ammonium bifluoride paste. This method was tried but the scratching of the precise pattern on the wax was found to be too laborious with too high a probability of breakage for the thin cover glasses used.

As an alternative, a teflon clamp was machined which covered the glass in the spots to be etched. The glass and the teflon clamp were then dipped in molten wax. After solidification of the wax, the clamp was removed exposing the glass part to be etched. However, the wax strongly adhered in the areas between the glass and the edge of the clamp and removing it caused breaking of the glass.

An additional problem associated with the use of wax was encountered during etching. It was found that HF would penetrate under the wax. Two waxes were tried: paraffin and black Apiezon. The penetration problem occurred with both of these.

Photo-Resist Mask and Etch

The use of photo-resist techniques to mask the glass for etching was investigated. Two photo-resist materials were used which could be removed in a developer after irradiation with ultraviolet. This is a standard method used in microelectronics. The photo-resists were: 1) Hunts photo-resist which is soluble in hot H_2SO_4 and 2) Shipley photo-resist which is soluble in acetone. Neither could stand HF or ammonium bifluoride. A primer sold by Shipley was also tried but it did not improve the adhesion of the photo-resist to the glass.

The process was as follows. The microsheet was placed on a vacuum chuck of a turntable. A few drops of primer were deposited in the middle of the glass which was then spun to distribute the primer evenly over the surface. After drying, the photo-resist was applied in the same way. After drying, the procedure was repeated on the other side of the glass cover. Next, the samples were "soft" baked and the glass was irradiated for two minutes under a mask which did not cover the spots to be etched. The photo-resist was then developed. This procedure was abandoned as fairly unpromising since even if a suitable photo-resist material could be found, the many steps of glass handling were time consuming and lead to an undue risk of glass breakage.

Thick Film Excellor Resist (Red R-511-5K) Mask and Etch

A "ruby" mask was made as in the photo-resist technique. Using this mask a silk screen was prepared by a photolithographic technique. The glass cover was held in the silk screening substrate support by a vacuum chuck. A suitable padding was made from vinyl tape to cushion the glass.

In the process, the glass was first dried in a $150^\circ C$ oven to remove the surface water. The photo-resist was then applied through the silk screen mask. The microsheet was then removed by sliding it into a wire basket. After drying in the oven at $150^\circ C$ for 10 minutes, the coat was applied on the other side. The next step was etching in an HF plus ammonium bifluoride solution. After experimenting with different strengths of HF and ammonium bifluoride mixture, the best results were obtained with a 50 percent HF solution for two minutes. The photo-resist was then removed in a vapor degreaser using trichlorethylene. The residue left after degreasing was removed using a toothbrush and detergent with the glass held on a vacuum chuck. The results of this method and the

efficiency of the procedure looked promising; but when applied to large batches of glass to attain efficiency; the breakage rate was unacceptable.